MULTILAYERED PLATE ELEMENTS WITH NODE-DEPENDENT KINEMATICS FOR THE ANALYSIS OF COMPOSITE AND SANDWICH STRUCTURES

Multilayered plate elements with node-dependent kinematics for the analysis of composite and sandwich structures

S. Valvano, E. Carrera

MUL2 group at Department of Mechanical and Aerospace Engineering,
Politecnico di Torino, Turin, Italy

Keywords:
Multilayered plate elements, Node-dependent kinematics, Equivalent-Single-Layer, Global/local analysis, Layer-Wise

Author and address for Correspondence
Dr. Stefano Valvano
Research Assistant,
Department of Mechanical and Aerospace Engineering
Politecnico di Torino,
Corso Duca degli Abruzzi, 24,
10129 Torino, ITALY,
tel +39.011.546.6871, fax +39.011.564.6899
e-mail: stefano.valvano@polito.it

Abstract

In this work, a new plate finite element (FE) for the analysis of composite and sandwich plates is proposed. By making use of node-variable plate theory assumptions, the new finite element allows for the simultaneous analysis of different subregions of the problem domain with different kinematics and accuracy, in a global/local sense. In particular higher-order theories with an Equivalent-Single-Layer (ESL) approach are simultaneously used with advanced Layer-Wise (LW) models. As a consequence, the computational costs can be reduced drastically by assuming refined theories only in those zones/nodes of the structural domain where the resulting strain and stress states present a complex distribution. On the contrary, computationally cheaper, low-order kinematic assumptions can be used in the remaining parts of the plate where a localized detailed analysis is not necessary. The primary advantage of the present variable-kinematics element and related global/local approach is that no ad-hoc techniques and mathematical artifices are required to mix the fields coming from two different and kinematically incompatible adjacent elements, because the plate structural theory varies within the finite element itself. In other words, the structural theory of the plate element is a property of the FE node in this present approach, and the continuity between two adjacent elements is ensured by adopting the same kinematics at the interface nodes. According to the Unified Formulation by Carrera, the through-the-thickness unknowns are described by Taylor polynomial expansions with ESL approach and by Legendre polynomials with LW approach. Furthermore, the Mixed Interpolated Tensorial Components (MITC) method is employed to contrast the shear locking phenomenon. Several numerical investigations are carried out to validate and demonstrate the accuracy and efficiency of the present plate element, including comparison with various closed-form and FE solutions from the literature.

1 Introduction

The development of new materials for advanced engineering applications leads to complex the analysis of layered structures in practice. This is mainly due to the complex anisotropy that characterizes this kind of structures and that leads to intricate mechanical phenomena. In some cases, structures may contain regions where three-dimensional (3D) stress fields occur. To accurately capture these localized 3D stress states, solid models or higher-order theories are necessary. The Finite Element Method (FEM) has a predominant role among the computational techniques implemented for the analysis of layered structures. The majority of FEM theories available in the literature are formulated by axiomatic-type theories. The conventional FEM plate model is the classical Kirchhoff-Love theory, and some examples are given in [1, 2], whose extension to laminates is known to as the Classical Lamination Theory (CLT) [3]. Another classical plate element is based on the First-order Shear Deformation Theory (FSDT), which rely on the works by Reissner [4] and Mindlin [5]. To overcome the limitations of classical theories, a large variety of plate finite element implementations of higher-order theories (HOT) have been proposed in the last years. HOT-based C^0 finite elements (C^0 means that the continuity is required only for the unknown variables and not for their derivatives) were discussed by Kant *et al.* [6] and Kant and Kommineni [7]. Many other papers are available in which HOTs have been implemented for plates, and more details can be found in the books from Reddy [8] and Palazotto and Dennis [9]. The HOT type theories presented are ESL models, the variables are indipendent from the number of layers. Differently the LW models permit to consider different sets of variables per each layer. A finite element implementations of Layer-Wise (LW) theories in the framework of axiomatic-type theories have been proposed by many authors, among which Noor and Burton [10], Reddy [11], Mawenya and Davies [12], Rammerstorfer et al. [13].

However, the high computational costs represent the drawback of refined plate theories or three-dimensional analyses. In recent years considerable improvements have been obtained towards the

implementation of innovative solutions for improving the analysis efficiency for a global/local scenario. In this manner, the limited computational resources can be distributed in an optimal manner to study in detail only those parts of the structure that require an accurate analysis. In general, two main approaches are available to deal with a global/local analysis: refining the mesh or the FE shape functions in correspondence with the critical domain; formulating multi-model methods, in which different subregions of the structure are analysed with different mathematical models. The coupling of coarse and refined mesh can be addressed as single-theory or single-model methods, and many techniques are present in literature [14, 15, 16]. In general, multi-theory methods can be divided into sequential or multistep methods, and simultaneous methods. In a sequential multi-model, the global region is analysed with an adequate model with a cheap computational cost to determine the displacement or force boundary conditions for a subsequent analysis at the local level. The local region can be modeled with a more refined theory, or it can be modeled with 3-D finite elements, see [17, 18, 19, 20]. The simultaneous multi-model methods are characterized by the analysis of the entire structural domain, where different subregions are modeled with different mathematical models and/or distinctly different levels of domain discretization, in a unique step. One of the simplest type of simultaneous multi-model methods for composite laminates analysis, is the concept of selective ply grouping or sublaminates [21, 22, 23]. In the literature, the local region (i.e., the region where accurate stress analysis is desired) is generally modeled by using 3-D finite elements in the domain of selective ply grouping method. Recently, the authors developed multi-model elements with variable through-the-thickness approximation by using 2-D finite elements for both local and global regions [24, 25, 26]. In this approach, the continuity of the primary variables between local and global regions was straightforwardly satisfied by employing Legendre polynomials. Another well-known method to couple incompatible kinematics in multi-model methods, is the use of Lagrange multipliers, which serve as additional equations to enforce compatibility between adjacent subregions. In the three-field formulation by Brezzi and Marini [27], an additional grid at the interface is introduced. The unknowns are represented independently in each sub-domain and at the interface, where the matching is provided by suitable Lagrange multipliers. This method was recently adopted by Carrera et al. [28, 29, 30] to couple beam elements of different orders and, thus, to develop variable kinematic beam theories. Ben Dhia *et al.* [31, 32, 33, 34] proposed the Arlequin method to couple different numerical models by means of a minimization procedure. This method was adopted by Hu *et al.* [35, 36] for the linear and non-linear analysis of sandwich beams modelled via one-dimensional and two-dimensional finite elements, and by Biscani *et al.* [37] for the analysis of beams and by Biscani *et al.* [38] for the analysis of plates. Reddy and Robbins [39] and Reddy [40] presented a multiple-model method on the basis of a variable kinematic theory and on mesh superposition in the sense of Fish [41] and Fish and Markolefas [42]. Coupling was obtained by linking the FSDT variables, which are present in all the considered models, without using Lagrangian multipliers. The coupling of different kinematics model in the framework of composite beam structure, using the extended variational formulation (XVF), is presented in [43], sinus model and classical kinematics are coupled into non-overlapping domains. In the present work, a new simultaneous multiple-model method for 2D elements with node-dependent kinematics is developed. This node-variable capability enables one to vary the kinematic assumptions within the same finite plate element. The expansion order of the plate element is, in fact, a property of the FE node in the present approach. Therefore, between finite elements, the continuity is ensured by adopting the same expansion order in the nodes at the element interface. This node-dependent finite element has been used by the authors in [44] using classical and HOT-type theories, Taylor polynomials were used with an ESL approach. The novelty of the present work state into the combination of HOT-type and advanced LW theories in the same finite element. In this manner, global/local models can be formulated without the use of any mathematical artifice. As a consequence, computational costs can be reduced assuming refined models only in those zones with a quasi-three-dimensional stress field, whereas computationally cheap, low-order kinematic assumptions are used in the remaining parts of the plate structure. In this paper, the governing equations of the

node-variable kinematic plate element for the linear static analysis of composite structures are derived from the Principle of Virtual Displacement (PVD). Subsequently, FEM is adopted and the Mixed Interpolation of Tensorial Components (MITC) method [45, 46, 47, 48] is used to contrast the shear locking. The developed methodology is, therefore, assessed and used for the analysis of multilayered cantilevered plates with concentrated loads, cross-ply plates with simply-supported edges and subjected to a localized pressure load, and unsimmetric laminated sandwich plates simply-supported and subjected to a localized pressure load. The results are compared with various theories and, whenever possible, with exact solutions available from the literature.

2 Refined and hierarchical theories for plates

In this work, different kinematic assumptions in different subregions of the problem domain are made by a new finite element which allows simultaneous multi-model analysis, without ad-hoc techniques and mathematical artifices, that usually are required to mix the fields coming from two different kinematic models. The present plate structural theory varies within the finite element itself.
To highlight the capabilities of the present formulation, a four-node plate elements with node-dependent kinematics is shown in Figure 1. The element proposed in this example makes use of a Layer-Wise theory of the first order at node 1. On the other hand, a second-order refined theory are employed at node 2. At node 3, a third order expansion is adopted. Finally, a Layer-Wise theory of the second order is assumed at node 4. As it will be clear later in this paper, the choice of the nodal plate theory is arbitrary and node-variable kinematic plate elements will be used to implement multi-model methods for global-local analysis. Before discussing the present formulation, a brief overview of refined and advanced plate theories is given below or the sake of completeness. Plates are bi-dimensional structures in which one dimension (in general the thickness in the z direction) is negligible with respect to the other two dimensions. The geometry and the reference system that is adopted throughout the present work are shown in Figure 1.

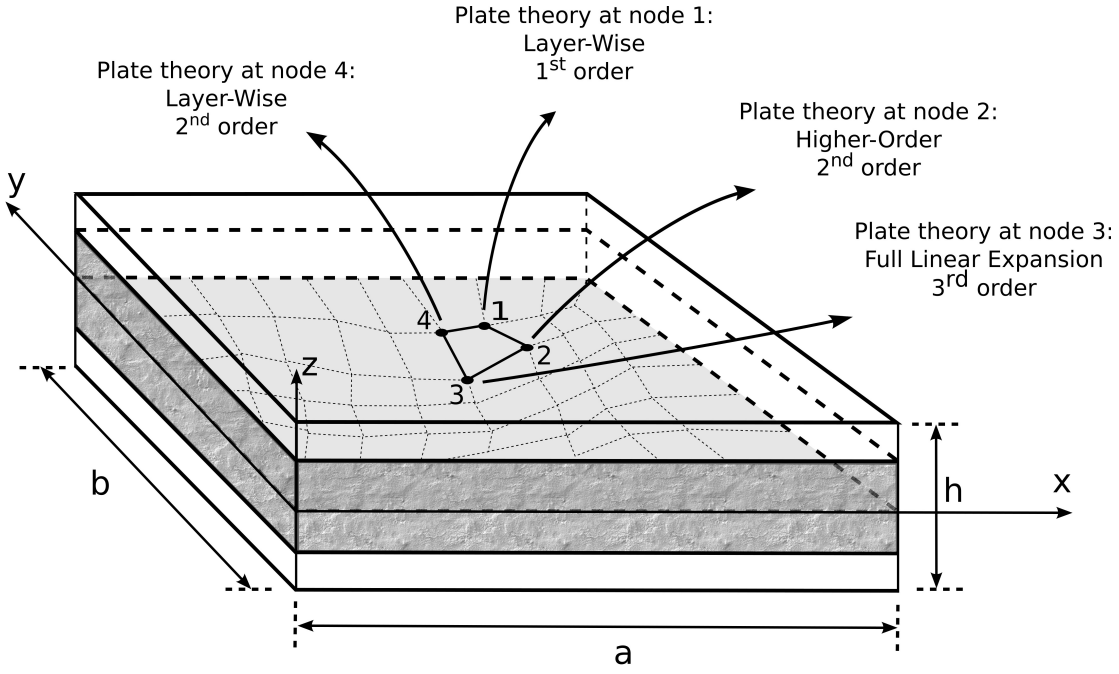

Figure 1: Example of sandwich structure described by plate element with node-dependent kinematics.

2.1 Higher-Order Theories

In order to overcome the limitations of classical theories, a large variety of plate higher-order theories (HOT) have been proposed in the past and recent literature. As a general guideline, it is clear that the richer the kinematics of the theory, the more accurate the 2D model becomes. HOT-type theories can be expressed by making use of Taylor-like expansions of the generalized unknowns along the thickness to formulate Equivalent-Single-Layer (ESL) models. In the case of generic expansions of N terms, HOT displacement field can be expressed as in Equation 1. For example, if a parabolical expansion order is taken into account, a graphical representation of a deflection can be depicted as in Figure 2a. Moreover, Figure 2b pictorially shows the capabilities of a generical HOT model, which can address complex kinematics in the thickness direction.

$$\begin{aligned} u(x,y,z) &= u_0(x,y) + z\,u_1(x,y) + ... + z^N\,u_N(x,y) \\ v(x,y,z) &= v_0(x,y) + z\,v_1(x,y) + ... + z^N\,v_N(x,y) \\ w(x,y,z) &= w_0(x,y) + z\,w_1(x,y) + ... + z^N\,w_N(x,y) \end{aligned} \tag{1}$$

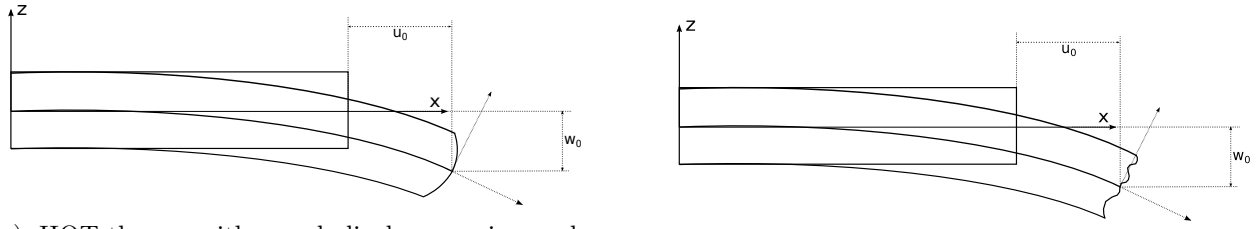

(a) HOT-theory with parabolical expansion order $N = 2$

(b) HOT-theory with generical expansion order

Figure 2: Geometrical representation of the Higher Order Theories.

For the sake of completeness, the classical models, Classical Lamination Theory (CLT) [1, 2, 3] and First-order Shear Deformation Theory (FSDT) [4], [5] kinematics, are particular cases of the full linear expansion, obtained from 1 imposing $N = 1$. For more details see [49]. Therfore, it is well known in literature that linear models are affected by the problem of the Poisson Locking (PL) phenomena. The remedy for the Poisson locking, except to use higher-order theories, is to modify the Elastic Coefficients of the material. The PL phenomena originates from constitutive laws which state the intrinsic coupling between in- and out-of-plane strain components. Classical plate theories correct the locking phenomena by imposing that the out-of-plane normal stress is zero. This hypothesis yields reduced material stiffness coefficients which have to be accountend in the Hooke law. Therefore, in literature, the correction of the material coefficients does not have a consistent theoretical proof. This means that the adoption of reduced material coefficients does not necessarily lead to the exact 3D solution, as shown in [50]. For the sake of clarity and simplicity of the present method explanation, the results presented in this work, with the full linear expansion kinematics, are not corrected for the PL phenomena.

2.2 The Unified Formulation framework

According to Unified Formulation by Carrera [49, 51, 52, 53], refined models can be formulated in a straightforward manner by assuming an expansion of each of the primary variables by arbitrary

functions in the thickness direction. Thus, each variable can be treated independently from the others, according to the required accuracy. This procedure becomes extremely useful when multifield problems are investigated such as thermoelastic and piezoelectric applications [54, 55, 56, 57]. In a displacement-based formulation, in fact, that the three-dimensional displacement field is the combination of through-the-thickness functions weighted by the generalized unknown variables:

$$\begin{aligned} u(x,y,z) &= F_0(z)\, u_0(x,y) + F_1(z)\, u_1(x,y) + ... + F_N(z)\, u_N(x,y) \\ v(x,y,z) &= F_0(z)\, v_0(x,y) + F_1(z)\, v_1(x,y) + ... + F_N(z)\, v_N(x,y) \\ w(x,y,z) &= F_0(z)\, w_0(x,y) + F_1(z)\, w_1(x,y) + ... + F_N(z)\, w_N(x,y) \end{aligned} \tag{2}$$

Similarly, in a compact form one has:

$$\boldsymbol{u}(x,y,z) \ = F_s(z)\boldsymbol{u}_s(x,y) \qquad s = 0,1,...,N \tag{3}$$

where $\boldsymbol{u}(x,y,z)$ is the three-dimensional displacement vector, $\boldsymbol{u}(x,y,z) = [u,v,w]$; F_s are the thickness functions depending only on z; $\boldsymbol{u}_s$ is the generalized displacement vector of the variables; s is a sum index; and N is the number of terms of the theory expansion. Depending on the choice of the thickness functions, F_s, and the number of terms in the plate kinematics, N, various theories can be implemented.

2.3 Advanced Theories

The ESL models formulated with Taylor-like thickness functions, however, may not be sufficiently accurate to describe adequately the multilayered structures in which, due to their intrinsic anisotropy, the first derivative of the displacement variables in the z-direction is discontinuous. Nevertheless, it is possible to reproduce the zig-zag effects in the ESL models by modifying opportunely the F_s functions, for example by adding the Murakami functions [58, 59]. On the other hand, plate models with Layer-Wise (LW) capabilities can be implemented by describing the displacement components at the layer level, possibly by using a combination of Lagrange and Legendre-like polynomial as F_s thickness functions [60, 61]. In the case of Layer-Wise (LW) models, the displacement is defined at k-layer level:

$$\begin{aligned} &\boldsymbol{u}^k(x,y,z) = \ F_t(z)\ \boldsymbol{u}_t^k(x,y) \ + \ F_b(z)\ \boldsymbol{u}_b^k(x,y) \ + \ F_r(z)\ \boldsymbol{u}_r^k(x,y) \ = \ F_s(z)\ \boldsymbol{u}_s^k(x,y) \\ &s = t,b,r \qquad r = 2,...,N \end{aligned} \tag{4}$$

$$F_t = \frac{P_0 + P_1}{2} \qquad F_b = \frac{P_0 - P_1}{2} \qquad F_r = P_r - P_{r-2} \tag{5}$$

in which $P_j = P_j(\zeta_k)$ is the Legendre polynomial of j-order defined in the ζ_k-domain: $-1 \leq \zeta_k \leq 1$. $P_0 = 1$, $P_1 = \zeta_k$, $P_2 = (3\zeta_k^2 - 1)/2$, $P_3 = (5\zeta_k^3 - 3\zeta_k)/2$, $P_4 = (35\zeta_k^4 - 30\zeta_k^2 + 3)/8$. The top ($t$) and bottom ($b$) values of the displacements are used as unknown variables and one can impose the following compatibility conditions:

$$u_t^k = u_b^{k+1} \qquad k = 1, N_l - 1 \tag{6}$$

For example, if a parabolical expansion order is taken into account, a graphical representation of a deflection can be depicted as in Figure 3.

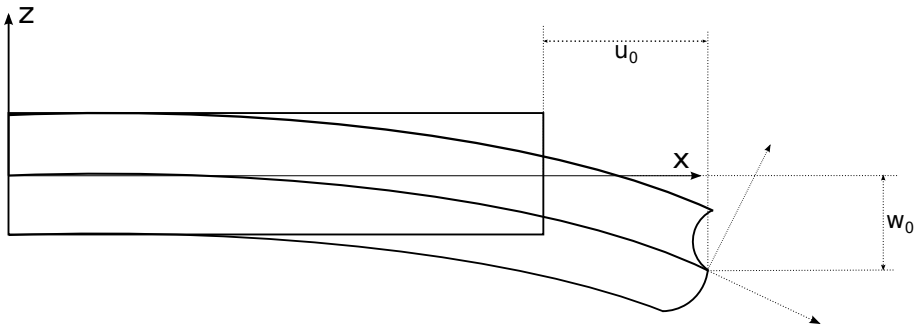

Figure 3: Geometrical representation of a parabolical layer-wise model deflection on a two layered plate.

3 Finite element approximation

3.1 Constitutive and geometrical relations for plates

The definition of the 3D constitutive equations permits to express the stresses by means of the strains. The generalized Hooke's law is considered, by employing a linear constitutive model for infinitesimal deformations. In a composite material, these equations are obtained in material coordinates $(1, 2, 3)$ for each orthotropic layer k and then rotated in the general reference system (x, y, z). Therefore, the stress-strain relations after the rotation, calculated for each layer k, are:

$$\boldsymbol{\sigma}^k = \boldsymbol{C}^k \, \boldsymbol{\epsilon}^k \tag{7}$$

where the stress and strain vectors have six components:

$$\begin{aligned} \boldsymbol{\sigma} &= [\sigma_{xx}, \, \sigma_{yy}, \, \sigma_{xy}, \, \sigma_{xz}, \, \sigma_{yz}, \, \sigma_{zz}] \\ \boldsymbol{\epsilon} &= [\epsilon_{xx}, \, \epsilon_{yy}, \, \epsilon_{xy}, \, \epsilon_{xz}, \, \epsilon_{yz}, \, \epsilon_{zz}] \end{aligned} \tag{8}$$

and $\boldsymbol{C}$ is the material elastic coefficients matrix defined as follows:

$$\boldsymbol{C} = \begin{bmatrix} C_{11} & C_{12} & C_{16} & 0 & 0 & C_{13} \\ C_{12} & C_{22} & C_{26} & 0 & 0 & C_{23} \\ C_{16} & C_{26} & C_{66} & 0 & 0 & C_{36} \\ 0 & 0 & 0 & C_{55} & C_{45} & 0 \\ 0 & 0 & 0 & C_{45} & C_{44} & 0 \\ C_{13} & C_{23} & C_{36} & 0 & 0 & C_{33} \end{bmatrix} \tag{9}$$

For the sake of brevity, the expressions that relate the material coefficients C_{ij} to the Young's moduli E_1, E_2, E_3, the shear moduli G_{12}, G_{13}, G_{23} and Poisson ratios ν_{12}, ν_{13}, ν_{23}, ν_{21}, ν_{31}, ν_{32} are not given here. They can be found in many reference texts, such as [11].
The geometrical relations enable one to express the strain vector $\boldsymbol{\epsilon}$ in terms of the displacement vector $\boldsymbol{u}$ for each layer k:

$$\boldsymbol{\epsilon}^k = \boldsymbol{D}_g \, \boldsymbol{u}^k \tag{10}$$

where $\boldsymbol{D}_g$ is the geometrical vector containing the differential operators defined as follows:

$$\boldsymbol{D}_g = \begin{bmatrix} \dfrac{\partial}{\partial_x} & 0 & 0 \\ 0 & \dfrac{\partial}{\partial_y} & 0 \\ \dfrac{\partial}{\partial_y} & \dfrac{\partial}{\partial_x} & 0 \\ \dfrac{\partial}{\partial_z} & 0 & \dfrac{\partial}{\partial_x} \\ 0 & \dfrac{\partial}{\partial_z} & \dfrac{\partial}{\partial_y} \\ 0 & 0 & \dfrac{\partial}{\partial_z} \end{bmatrix} \tag{11}$$

3.2 Node-dependent kinematics for plate finite elements

By utilizing an FEM approximation, the generalized displacements of Equation (3) can be expressed as a linear combination of the shape functions to have

$$\boldsymbol{u}_s(x,y) = N_j(x,y)\boldsymbol{u}_{s_j} \qquad j = 1, ..., (\text{nodes per element}) \tag{12}$$

where $\boldsymbol{u}_{s_j}$ is the vector of the generalized nodal unknowns and N_j can be the usual Lagrange shape functions. j denotes a summation on the element nodes. Since the principle of virtual displacements in used in this paper to obtain the elemental FE matrices, it is useful to introduce the finite element approximation of the virtual variation of the generalized displacement vector $\delta\boldsymbol{u}_\tau$,

$$\delta\boldsymbol{u}_\tau(x,y) = N_i(x,y)\delta\boldsymbol{u}_{\tau_i} \qquad i = 1, ..., (\text{nodes per element}) \tag{13}$$

In Eq. (13), δ denotes the virtual variation, whereas indexes τ and i are used instead of s and j, respectively, for the sake of convenience.

In this work, and according to Eqs. (3), (12) and (13), the thickness functions F_s and F_τ, which determine the plate theory order, are independent variables and may change for each node within the plate element. Namely, the three-dimensional displacement field and the related virtual variation can be expressed to address FE node-dependent plate kinematics as follows:

$$\begin{aligned} \boldsymbol{u}(x,y,z) &= F_s^j(z)N_j(x,y)\boldsymbol{u}_{s_j} \qquad s = 0,1,...,N^j \quad j = 1, ..., (\text{nodes per element}) \\ \delta\boldsymbol{u}(x,y,z) &= F_\tau^i(z)N_i(x,y)\delta\boldsymbol{u}_{\tau_i} \quad \tau = 0,1,...,N^i \quad i = 1, ..., (\text{nodes per element}) \end{aligned} \tag{14}$$

where the subscripts τ, s, i, and j denote summation. Superscripts i and j denote node dependency, such that for example F_τ^i is the thickness expanding function and N^i is the number of expansion terms at node i, respectively. As example, the displacement field of the node-variable kinematic plate element as discussed in Figure 1 is described in detail hereafter. The global displacement field of the element is approximated as follows:

- Node 1 Plate Theory = LW with $N^1 = 1$ Eq. (4)
- Node 2 Plate Theory = HOT with $N^2 = 2$ Eq. (1)
- Node 3 Plate Theory = HOT with $N^3 = 3$ Eq. (1)
- Node 4 Plate Theory = LW with $N^4 = 2$ Eq. (4)

According to Equation 14, it is easy to verify that the displacements at a generic point belonging to the plate element can be expressed as given in Equation 15. In this equation, only the displacement component along x-axis is given for simplicity reasons:

$$\begin{aligned} u(x,y,z) = &\left[\left(\frac{1+\zeta}{2}\right) u_{0_1} + \left(\frac{1-\zeta}{2}\right) u_{1_1}\right] N_1(x,y) + \left(u_{0_2} + z\, u_{1_2} + z^2\, u_{2_2}\right) N_2(x,y) + \\ &+ \left(u_{0_3} + z\, u_{1_3} + z^2\, u_{2_3} + z^3\, u_{3_3}\right) N_3(x,y) + \left[\left(\frac{1+\zeta}{2}\right) u_{0_4} + \left(\frac{1-\zeta}{2}\right) u_{1_4} + \left(\frac{3(\zeta^2-1)}{2}\right) u_{2_4}\right] N_4(x,y) \end{aligned} \tag{15}$$

It is intended that, due to node-variable expansion theory order, the assembling procedure of each finite element increases in complexity with respect to classical mono-theory finite elements. In order to simplify the description of the assembling procedure, tthe governing equations are developed in form of fundamental nucleus, as described below.

3.3 Governing equations and fundamental nucleus

The governing equations for the static response analysis of the multi-layer plate structure can be obtained by using the principle of virtual displacements, which states:

$$\int_{\Omega}\int_{A} \delta\boldsymbol{\epsilon}^T \boldsymbol{\sigma}\; d\Omega\, dz = \delta L_e \tag{16}$$

where the term on the left-hand side represents the virtual variation of the strain energy; Ω and A are the integration domains in the plane and the thickness direction, respectively; $\boldsymbol{\epsilon}$ and $\boldsymbol{\sigma}$ are the vector of the strain and stress components; and δL_e is the virtual variation of the external loadings. By substituting the constitutive equations for composite elastic materials Equation 7, the linear geometrical relations Equation 10 as well as Equation 14 into Equation 16, the linear algebraic system in the form of governing equations is obtained in the following matrix expression:

$$\delta\boldsymbol{u}_{\tau_i}: \quad \boldsymbol{K}^{\tau sij}\boldsymbol{u}_{s_j} = \quad \boldsymbol{P}^{\tau i} \tag{17}$$

where $\boldsymbol{K}^{\tau sij}$ and $\boldsymbol{P}^{\tau i}$ are the element stiffness and load FE arrays written in the form of *fundamental nuclei*. The explicit expressions of the *fundamental nuclei* for node-dependent variable kinematic plate elements is given in [44]. It must be added that, in this work, an MITC technique is used to overcome the shear locking phenomenon, see [57]. The fundamental nucleus is the basic building block for the construction of the element stiffness matrix. In fact, given these nine components, element stiffness matrices of arbitrary plate models can be obtained in an automatic manner by expanding the fundamental nucleus versus the indexes τ, s, i, and j. In the present FE approach, the node-dependent variable kinematic model, it is clear that both rectangular and square arrays are handled and opportunely assembled for obtaining the final elemental matrices. In the development of ESL and LW theories, the fundamental nucleus of the stiffness matrix is evaluated at the layer level and then assembled as shown in Figure 4. This figure, in particular, illustrates the expansion of the fundamental nucleus in the case of a 9-node Lagrange finite element with node-by-node variable kinematics, as in the case of this paper. However, for more details about the explicit formulation of the Unifide Formulation fundamental nuclei, interested readers are referred to the recent book by Carrera *et al.* [49].

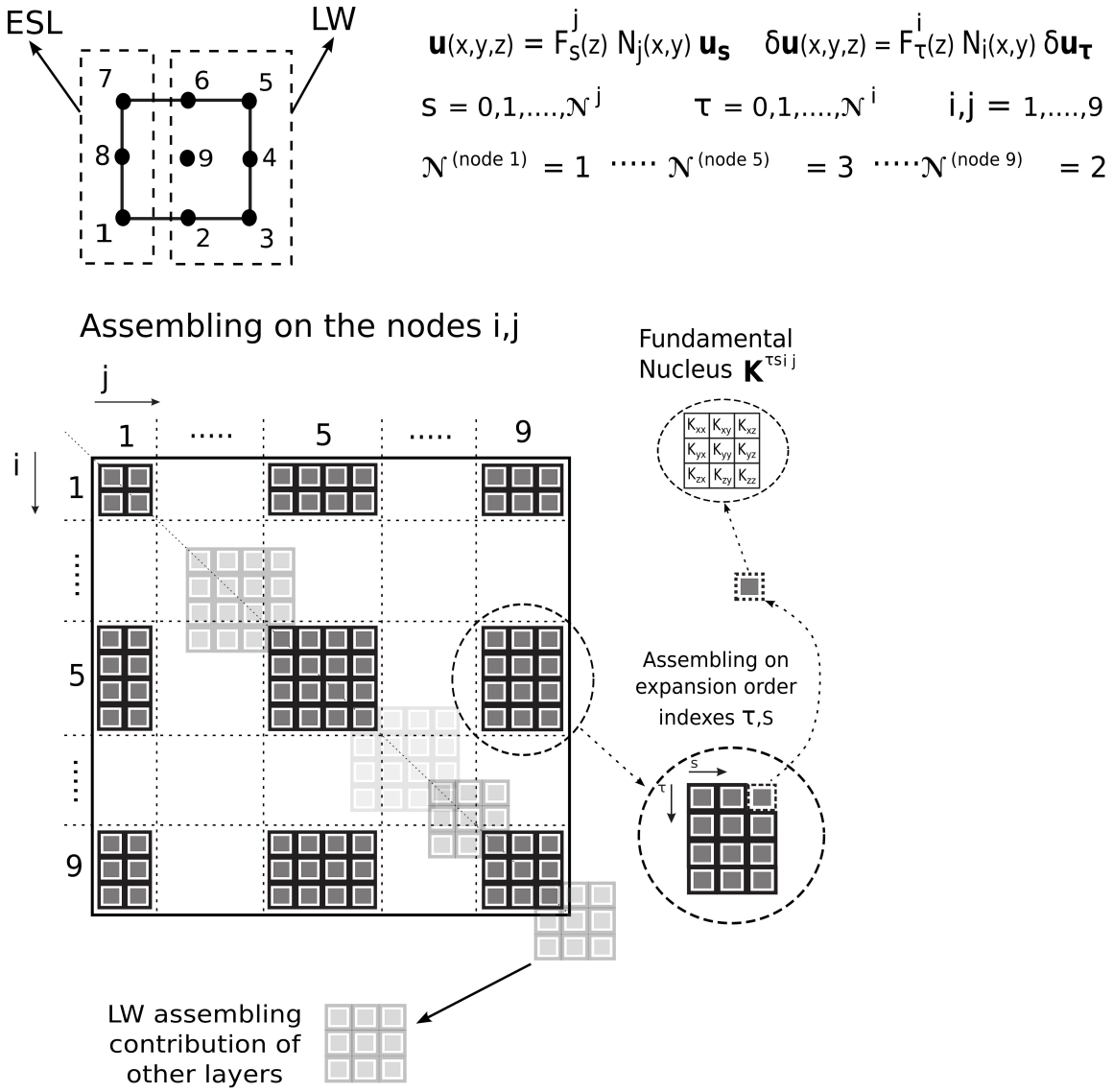

Figure 4: Assembling scheme of a 9-node finite element with node-dependent kinematics. Highlights of the influence of the LW contribution of other layers in the FE stiffness.

4 Numerical results

In this numerical section some problems have been considered to assess the capabilities of the proposed node-variable kinematic plate elements and related global/local analysis. These analysis cases comprise composite laminated and sandwich plate structures with different boundary conditions and loadings. Whenever possible, the proposed multi-theory models are compared to single-theory refined elements. The acronyms for the ESL models are indicated with the first letter E, the second letter indicates the polynomial kind, T for Taylor polynomials and L for Legendre polynomials. The LW models are indicated with the letters LW. The third letter indicates the number of the theory approximation order. If the analytical Navier solution type is employed, a subscript a is added. Moreover, analytical solution with higher-order single models, and multi-model theories present in literature are given for some cases. For the sake of clarity, present multi-model theories are opportunely described for each numerical case considered.

4.1 Eight-layer cantilever plate

The first structure case taken into account is a simple example, that easily permits to describe, through the results, the main capabilities of the present node-dependent plate element. A cantilever eight-layer plate is analysed as shown in Figure 5. The structure is loaded at the free end with a concentrated load equal to $P_z = -0.2\,N$. The geometrical dimensions are: $a = 90\,mm$, $b = 1\,mm$, $h = 10\,mm$. The mechanical properties of the material labeled with the number 1 are: $E_L = 30\,GPa$, $E_T = 1\,GPa$, $G_{LT} = G_{TT} = 0.5\,GPa$, $\nu_{LT} = \nu_{TT} = 0.25$. On the other hand, the mechanical properties of the material labeled with the number 2 are: $E_L = 5\,GPa$, $E_T = 1\,GPa$, $G_{LT} = G_{TT} = 0.5\,GPa$, $\nu_{LT} = \nu_{TT} = 0.25$. As clear from Figure 5, the material stacking sequence is $[1/2/1/2]_s$.
First, a convergence study on single-theory plate models was performed. For both $LW4$ and $ET4$ models, as shown in Table 1, a mesh grid of 12×2 elements is enough to ensure convergent results, for transverse mechanical displcement w, in-plane stress σ_{xx} and transverse normal stress σ_{xz}. Various node-variable kinematic plate models have been used to perform the global/local analysis of the proposed plate structure, and they are depicted in Figure 6. These models are compared in Table 2 with lower- to higher-order single-theory models as well as with various solutions from the literature, including an analytical solution based on the 2D elasticity as presented in Lekhnitskii [62].
It can be observed for the transverse displacements w that mono-theory LW models show a good accuracy solution indipendently of the polynomial order, differently for single-model ESL with Taylor polynomial yield good results only with higher-order expansion $ET3$ and $ET4$. Moreover multi-theory ESL models $Case\,A$, $Case\,B$ and $Case\,C$ show an intermediate solution accuracy for all the three considered cases without relevant differences. For the multi-theory ESL-LW models $Case\,D$, $Case\,E$ and $Case\,F$ the solution is very accurate, due to the partial LW approximation, and it is obtained exactly the same solution for the three considered cases.
Regarding the in-plane stress σ_{xx} the accuracy solution is not sensitive for all the considered single and multi model theories, except for the $Case\,A$ configuration where the transition elements are acting at the evaluation position.
For the transverse shear stress σ_{xz} similar comments respect to the transverse displacement can be drawn. Single theory LW models show a good accuracy solution indipendently of the polynomial order, otherwise higher-order mono-model ESL theories with Taylor polynomial, $ET3$ and $ET4$, are required to obtained a sufficient solution accuracy. Nevertheless, accurate solutions in localized regions/points can be obtained by using the multi-theory ESL model $Case\,B$, and with multi-theory ESL-LW models $Case\,D$ and $Case\,E$.

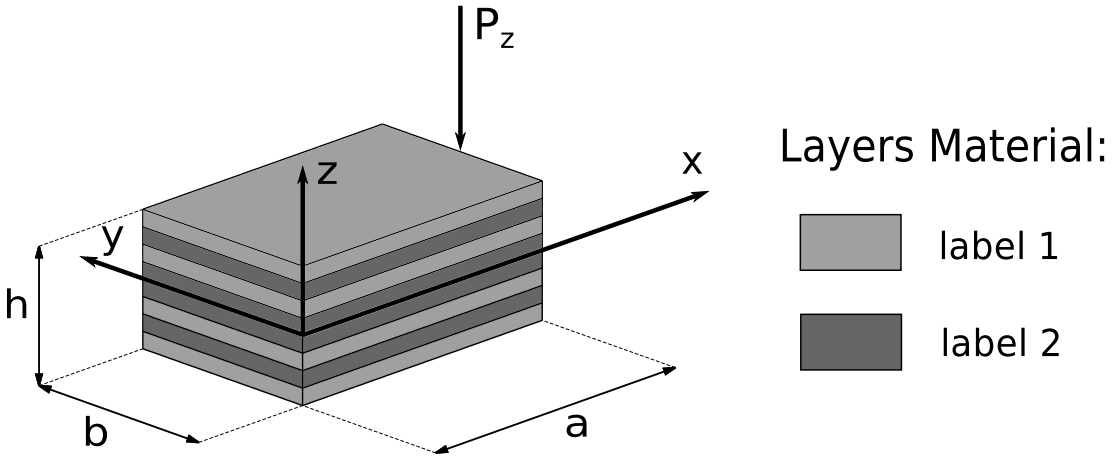

Figure 5: Eight-layered plate with concentrated loading. Reference system and material lamination scheme.

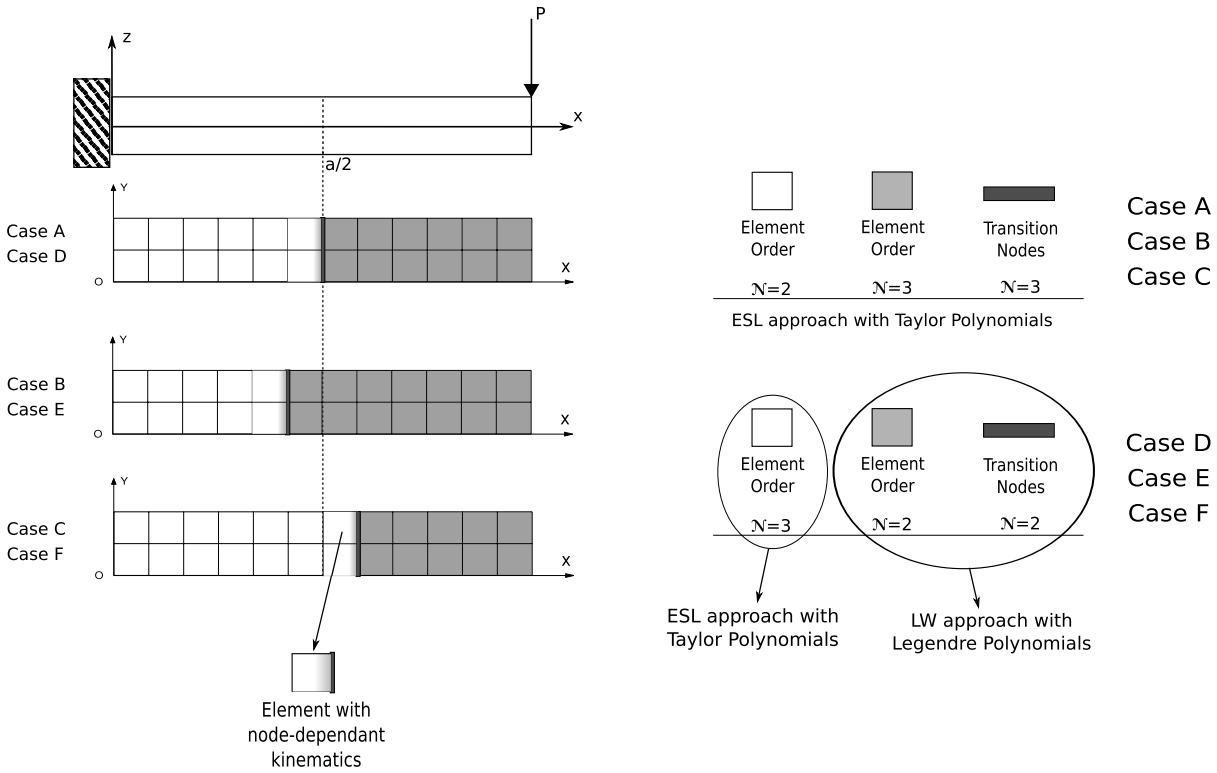

Figure 6: Eight-layered plate. Mesh scheme of the adopted multi-theory models with node-dependent kinematics.

Table 1: Convergence study of single-theory models of the eight-layer cantilever plate. Transverse displacement $w = -10^2 \times w(a, b/2, 0)$, in-plane principal stress $\sigma_{xx} = 10^3 \times \sigma_{xx}(a/2, b/2, +h/2)$, transverse shear stress $\sigma_{xz} = -10^2 \times \sigma_{xz}(a/2, b/2, 0)$.

	Mesh	2×2	4×2	6×2	8×2	10×2	12×2
$LW4$	w	3.031	3.032	3.031	3.030	3.030	3.030
	σ_{xx}	651	690	716	725	728	730
	σ_{xz}	2.991	2.797	2.792	2.791	2.790	2.789
$ET4$	w	3.029	3.029	3.029	3.028	3.028	3.028
	σ_{xx}	684	723	729	730	731	731
	σ_{xz}	3.054	2.829	2.820	2.821	2.822	2.822

Table 2: Eight-layer cantilever plate. Transverse displacement $w = -10^2 \times w(a, b/2, 0)$, in-plane normal stress $\sigma_{xx} = 10^3 \times \sigma_{xx}(a/2, b/2, +h/2)$, transverse shear stress $\sigma_{xz} = -10^2 \times \sigma_{xz}(a/2, b/2, 0)$ by various single- and multi-theory models.

	w	σ_{xx}	σ_{xz}	$DOFs$
Reference solutions				
Nguyen and Surana [63]	3.031	720		
Davalos *et al.* [64]	3.029	700		
Xiaoshan [65]	3.060	750		
Vo and Thai [66]	3.024			
Lekhnitskii [62]		730	2.789	
Present single- and multi-theory models				
$LW4$	3.030	730	2.789	12375
$LW3$	3.030	731	2.788	9375
$LW2$	3.030	731	2.795	6375
$LW1$	3.022	731	2.775	3375
$ET4$	3.028	731	2.822	1875
$ET3$	3.027	731	2.822	1500
$ET2$	2.980	731	2.005	1125
$ET1$	2.981	729	2.000	750
$Case\,A$	3.004	808	2.375	1320
$Case\,B$	3.010	737	2.781	1365
$Case\,C$	3.002	731	2.030	1305
$Case\,D$	3.028	732	2.799	4035
$Case\,E$	3.028	729	2.799	4425
$Case\,F$	3.028	731	2.818	3645

Some results in terms of transverse displacement w and transverse shear stress σ_{xz} along the thickness are represented in Figures 7a and 7b, 8a and 8b, respectively. Some more comments can be made:

- As shown in Figure 7a, the through-the-thickness distribution of the transverse displacement w, evaluated at the free tip of the plate, is correctly predicted by a third-order ESL model $ET3$. The same accuracy cannot be reached by the proposed ESL models with node-variable kinematics. Differently, as depicted in Figure 7b, both LW single theory and ESL-LW theory accuracy is not sensitive of the choosen model, except for the single linear model $LW1$.

- Figure 8a shows that the transverse shear stress σ_{xz}, evaluated at the mid-span of the plate, is very sensitive to the position of the transition variable-kinematic elements. $Case\,B$ model has the same accuracy as mono-model $ET3$ and $ET4$. On the contrary, the $Case\,C$ configuration has poor accuracy like mono-models $ET1$ and $ET2$. Finally, $Case\,A$ model presents a intermediate compromise between the other two multi-theory cases. All the ESL models are not able to reproduce the accurate behaviour of the reference 2D elasticity solution *Lekhnitskii*, presented in [62]. On the contrary, as depicted in Figure 8b, the LW single models are able to reach

an accurate solution as the reference solution *Lekhnitskii*, except for the linear model $LW1$. Multi-theory ESL-LW (ET3-LW2) models have a good approximation of the solution where the verification point is described by LW theories, *Case D* and *Case E* models, therefore *Case F* show the same accuracy solution of the model $ET3$.

By the evaluation of the various node-variable kinematic models, it is clear that an accurate representation of the stresses in localized zones is possible with DOFs reduction if an accurate distribution of the higher-order kinematic capabilities is performed in those localized zones. Differently, the displacements values are dependent on the global approximation over the whole structure. The DOFs reduction can be moderate or stronger, depending on the structure and the load case configuration.

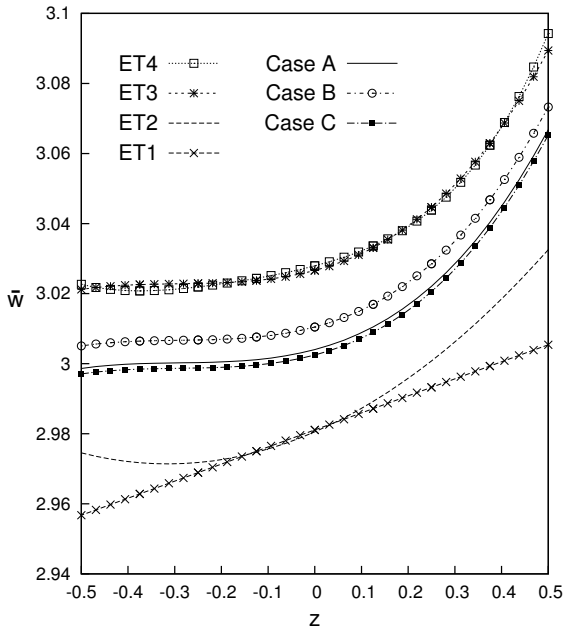

(a) ESL single and multi model with Taylor Polynomials

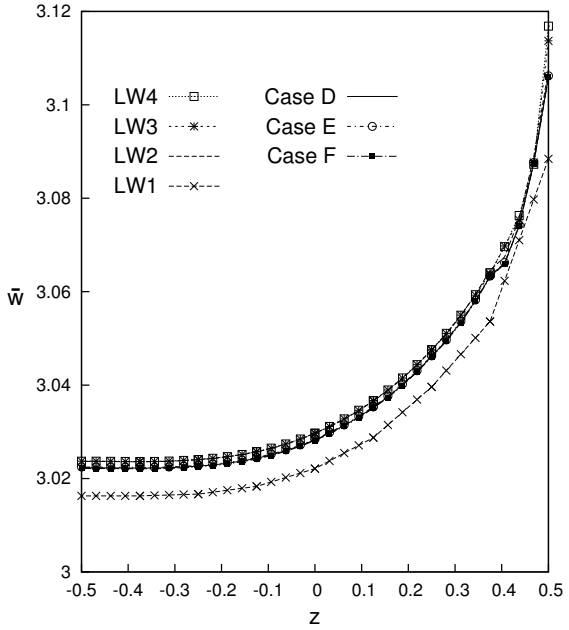

(b) LW single model, and multi-theories with ESL model by Taylor Polynomials combined with LW model by Legendre Polynomials

Figure 7: Eight-layer composite plate. Transverse displacement $w(x; y) = -10^2 \times w(a; b/2)$.

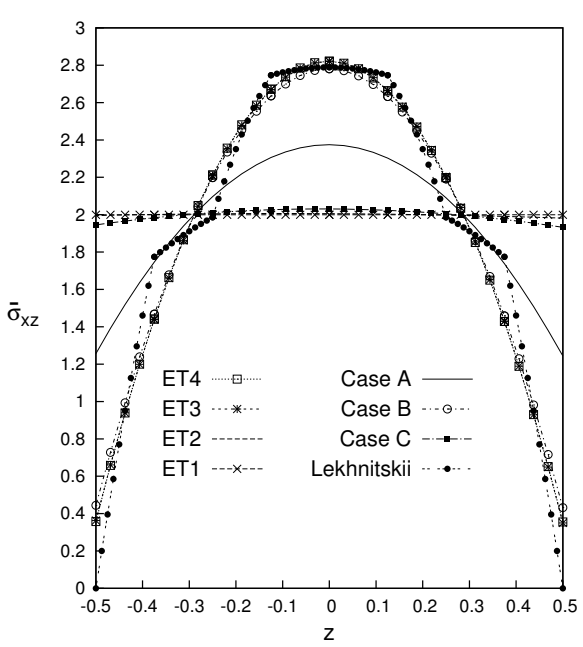

(a) ESL single and multi model with Taylor Polynomials

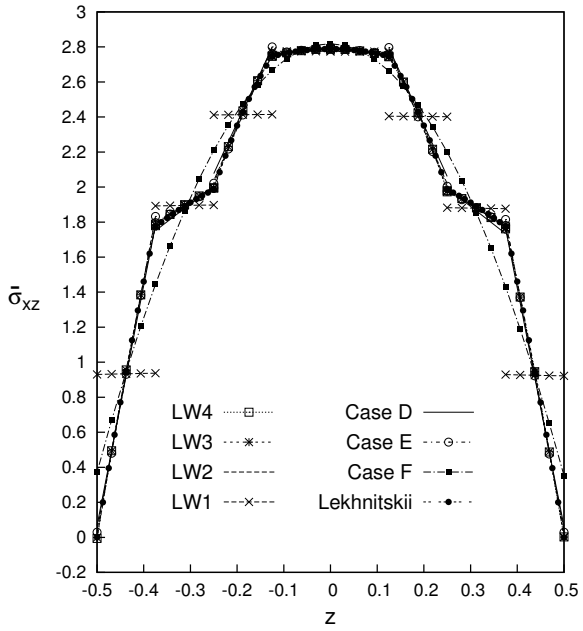

(b) LW single model, and multi-theories with ESL model by Taylor Polynomials combined with LW model by Legendre Polynomials

Figure 8: Eight-layer composite plate. Transverse shear stress $\sigma_{xz}(x;y) = -10^2 \times \sigma_{xz}(a/2;b/2)$.

4.2 Composite plates simply-supported

A simply-supported composite plate is analysed. The geometrical dimensions are: $a = b = 0.1\,m$, the side-thickness ratio is $a/h = 10$. A symmetric $[0°/90°/0°]$ stacking sequences is considered. The material employed is orthotropic with he following properties: $E_L = 132.5\,GPa$, $E_T = 10.8\,GPa$, $G_{LT} = 5.7\,GPa$, $G_{TT} = 3.4\,GPa$, $\nu_{LT} = 0.24$, $\nu_{TT} = 0.49$. The plate is simply-supported and a localised uniform transverse pressure, $P_z = -1\,MPa$, is applied at top face on a square region of side length equal to $a/5 \times b/5$ and centered at the point $(a/2, b/2)$, see Figure 9. In order to take into account other solutions present in literature [38] a non-uniform mesh grid of 20×20 elements ensures the convergence of the solution, taken from [44], and permits a fair comparison of the results. The non-uniform adopted mesh and the various node-variable kinematic models, with global/local capabilities used to perform the analysis of the proposed plate structure, are depicted in Figure 9, where the mesh grid of a quarter of the plate is analysed. Due to the simmetry of both the geometry and the load, a quarter of the plate is analyzed and the following symmetry and boundary conditions (simply-supported) are applied:

$$\begin{array}{cc} \textit{Boundary} & \textit{Simmetry} \\ u_s(x,0) = 0 \quad w_s(x,0) = 0 & u_s(a/2,y) = 0 \\ v_s(0,y) = 0 \quad w_s(0,y) = 0 & v_s(x,b/2) = 0 \end{array} \tag{18}$$

The results are given in terms of transverse displacement w and in-plane normal stresses σ_{xx}, σ_{yy} evaluated at $(a/2, b/2, -h/2)$, transverse shear stress σ_{xz} evaluated at $(5a/12, b/2, 0)$, and transverse normal stress σ_{zz} evaluated at $(a/2, b/2, +h/2)$.

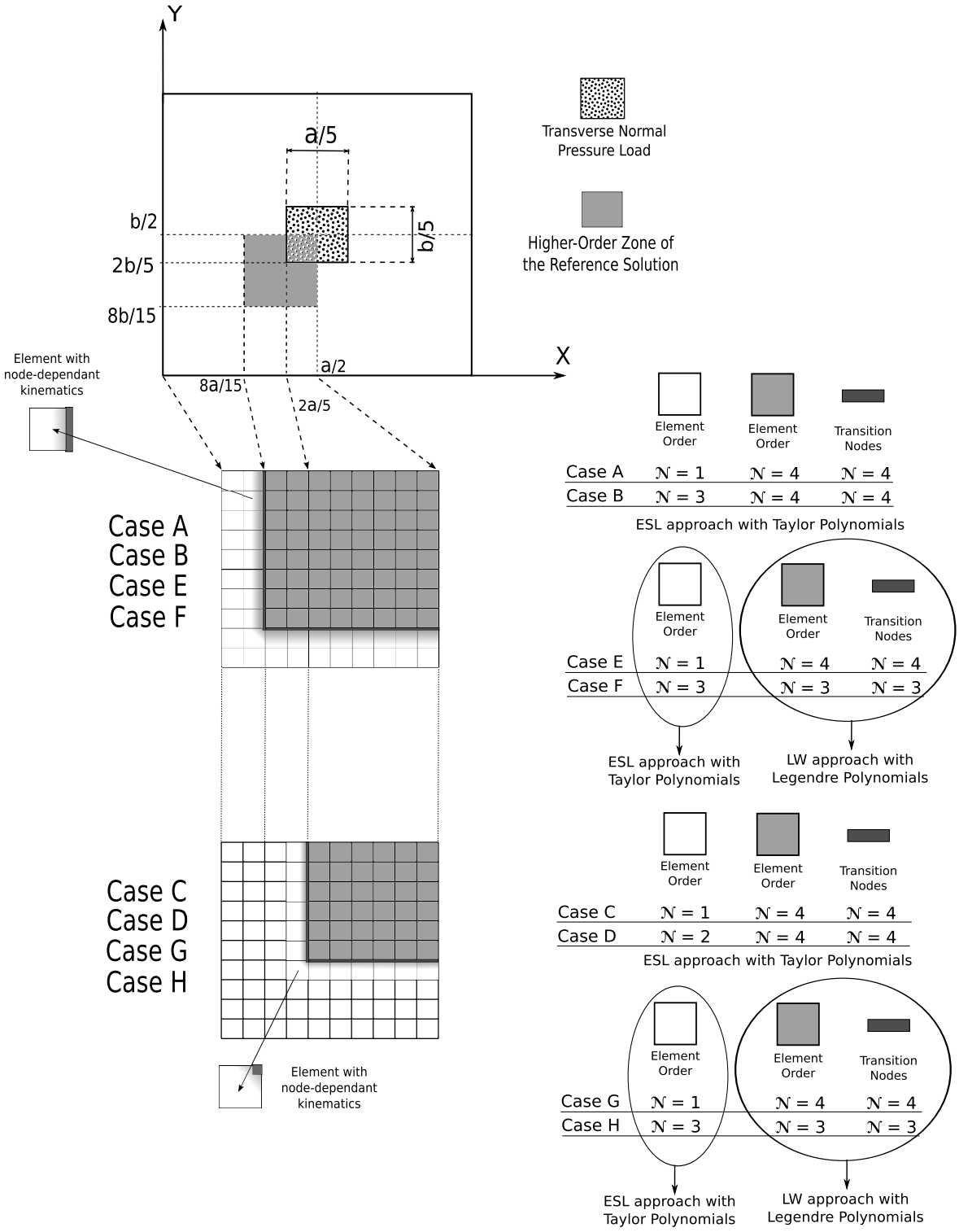

Figure 9: Non-uniform adopted mesh on quarter of the plate, and graphical representation of the multi-theory models of the cross-ply plate structure.

For the three-layered plate structure with $[0°/90°/0°]$, mono-theory models are compared with those from the present global/local approach in Table 3. The table shows that mono-theory ESL models with lower expansion order, $ET1$ and $ET2$, are not able to describe appropriately the transverse displacements w and the in-plane stresses σ_{xx} and σ_{yy}, otherwise LW mono-models represent these

variables with a good accuracy solution for every expansion order. To accurately describe the shear transverse stresses σ_{xz}, ESL higher-order theories are required, or LW mono-models theories. The transverse normal stress σ_{zz} needs higher-order theories to be well described, both linear ESL and LW single-models are not sufficient. Table 3 also show solutions for variable kinematic multi-model theories, the cases taken into account are named from $Case\,A$ to $Case\,H$, and they are explained in Figure 9. The cases named as $Case\,A$, $Case\,B$ and $Case\,E$ are equivalent to the models $(ET1-ET4)^A$, $(ET3-ET4)^B$ and $(ET1-LW4)^E$ taken from [38] and in which, via the Arlequin method and 4-node Lagrangian plate elements, a fourth-order plate theory is used in correspondence of the loading and a first- and third-order kinematics is used outside the loading zone, respectively.

Table 3: Composite plate with $[0°/90°/0°]$ lamination. Transverse displacement $w = (-10^5) \times w(a/2, b/2, -h/2)$, in-plane normal stresses $\sigma_{xx} = \sigma_{xx}(a/2, b/2, -h/2)$ and $\sigma_{yy} = \sigma_{yy}(a/2, b/2, -h/2)$, transverse shear stress $\sigma_{xz} = (-10) \times \sigma_{xz}(5a/12, b/2, 0)$, and transverse normal stress $\sigma_{zz} = -\sigma_{xz}(a/2, b/2, +h/2)$ by various single- and multi-theory models.

	w	σ_{xx}	σ_{yy}	σ_{xz}	σ_{zz}	$DOFs$
Reference solutions [38]						
$3D$	1.674	11.94	2.019	6.524		
$LW4_a$	1.675	11.94	2.020	6.523		39
$LW4$	1.672	11.83	1.983	6.464		9984
$ET4_a$	1.660	11.95	2.005	5.865		15
$ET4$	1.657	11.85	1.985	5.830		3840
$(ET1-ET4)^A$	1.609	11.92	1.962	5.848		2448
$(ET3-ET4)^B$	1.657	11.84	1.985	5.831		3936
$(ET1-LW4)^E$	1.617	11.91	1.953	6.481		3984
Present single- and multi-theory models						
$LW4$	1.6745	11.9547	2.0232	6.5557	1.0000	17199
$LW3$	1.6745	11.9624	2.0302	6.5613	1.0108	13230
$LW2$	1.6719	11.9141	2.0458	6.3903	1.0731	9261
$LW1$	1.6369	11.3621	2.1465	6.5881	1.4679	5292
$ET4$	1.6596	11.9556	2.0078	5.8473	0.9905	6615
$ET3$	1.6590	11.9867	2.1164	6.0147	1.2443	5292
$ET2$	1.5625	10.1942	1.7935	3.8521	1.0377	3969
$ET1$	1.4954	10.2867	2.1002	3.7554	1.8261	2646
$Case\,A$	1.6040	12.0084	1.9821	5.8510	0.9910	5247
$Case\,B$	1.6596	11.9556	2.0077	5.8473	0.9905	6159
$Case\,C$	1.5257	11.7328	1.9453	4.9414	0.9938	4167
$Case\,D$	1.5770	11.8056	1.9510	4.9970	0.9909	4983
$Case\,E$	1.6103	12.0107	1.9923	6.5254	1.0000	12183
$Case\,F$	1.6670	11.9699	2.0263	6.5524	1.0108	10494
$Case\,G$	1.5274	11.7105	1.9474	5.3212	1.0009	8223
$Case\,H$	1.6613	11.9305	2.0198	6.3616	1.0118	8334

Some results in terms of transverse displacement w, and transverse shear stress σ_{xz} along the thickness are represented in Figures 10a, 10b, 11a and 11b. The following remarks can be made:

- The transverse displacement w behaviour can change sensitively depending on the distribution of the kinematic enrichment within the structure plane. Figure 10a show that $Case\,B$ has the same accuracy as the full higher-order $ET4$ mono-model with a 8% DOFs reduction, and an accuracy

close to multi-model $Case\,H$ with a 26% DOFs reduction. It is noticeable that, the choice of the ESL or LW model for the loaded zone is not decisive for the correct description of the transverse mechanical displacement, as shown for $Case\,C$ and $Case\,G$. On the contrary a global more refined approximation get better accuracies, as the case of the multi-models $Case\,A$ and $Case\,E$.

- For the evaluation of the transverse shear stress σ_{xz}, higher-order models are necessary in the regions close to the considered evaluation point. In Figure 10b mono-model $LW4$ is used as reference solution. It is evident that ESL single-models, for every expansion orders, are not able to correctly describe the transverse shear stress. The ESL multi-model $Case\,A$ has the same poor accuracy of the theory $ET4$. The linear model $LW1$ is clearly not sufficient to describe the transverse shear stress, differently from the single value reported in Table 3 taken in $z = 0$. In Figure 11a the multi-model $Case\,E$ and $Case\,G$, where in the boundary regions a $ET1$ model is used and in the loaded zones a $LW4$ model is adopted, the accuracy on the transverse shear stress is not completely guaranteed by the LW model. In particular for the $Case\,G$ the evaluation point is close to the transition element, this position is perturbating the accuracy solution. On the contrary for the $Case\,E$ the evaluation point is not more close to the transition element and the solution accuracy is like the full LW model. Finally in Figure 11b the multi-model $Case\,F$ and $Case\,H$ are not suffering any perturbation poblem, due to the third-order ESL model of the boundary regions.

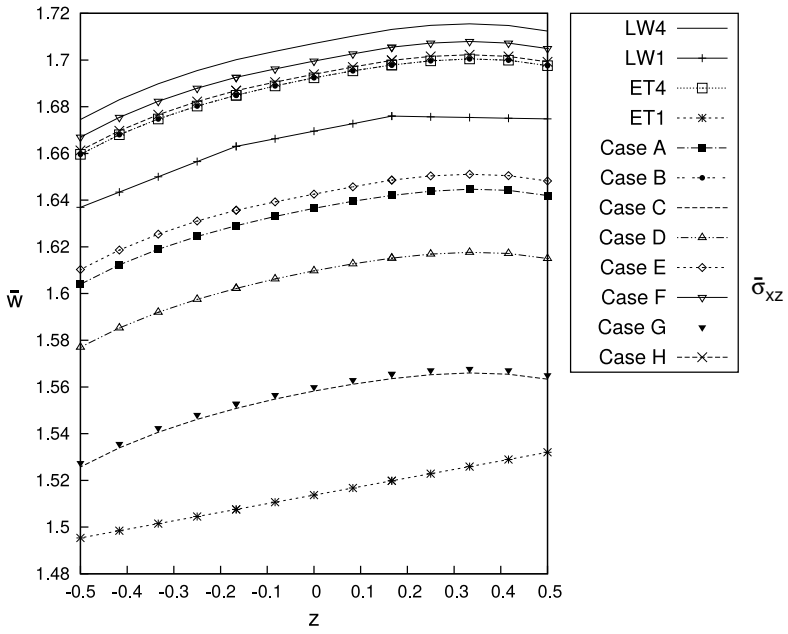

(a) Single and multi models

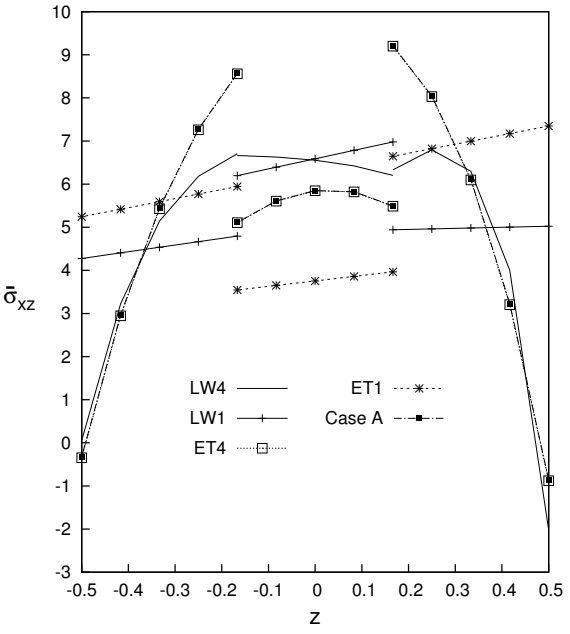

(b) ESL and LW single model, and ESL multi-model with Taylor Polynomials

Figure 10: Composite plate. Transverse displacement $w(x;y) = -10^5 \times w(a/2;b/2)$, and transverse shear stress $\sigma_{xz}(x;y) = -10 \times \sigma_{xz}(5a/12;b/2)$.

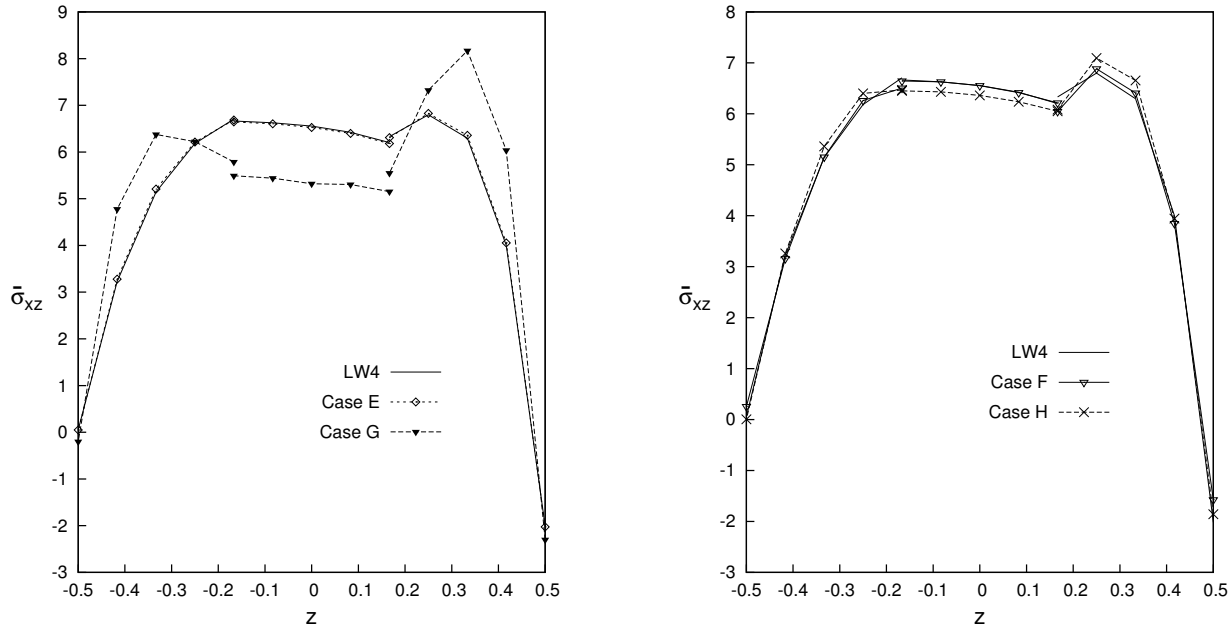

(a) (b)

Figure 11: Composite plate. Transverse shear stress $\sigma_{xz}(x;y) = -10 \times \sigma_{xz}(5a/12; b/2)$. Multi-theories with ESL model by Taylor Polynomials combined with LW model by Legendre Polynomials.

Results in terms of in-plane stress σ_{xx}, transverse shear stress σ_{xz} and transverse normal stress σ_{zz} along the in-plane x axis are represented in Figures 12a, 12b and 13a respectively.
For the in-plane stress σ_{xx}, see Figure 12a, the mono-models $LW4$ and $ET4$ show the same accuracy solution. Multi-models with ESL approach with Taylor polynomials, $Case\,A$ and $Case\,C$, produce small oscillations in the transition zone. On the contrary, multi-theories with ESL model by Taylor Polynomials combined with LW model by Legendre Polynomials, $Case\,E$ and $Case\,G$, show big fluctuations in the transition elements. Moreover it has to be noticed that if the refined polynomials are limited to the loading zone, $Case\,C$ and $Case\,G$, the solution accuracy in the loading zone is lower respect to the reference $LW4$ solution.
For the transverse shear stress σ_{xz}, see Figure 12b, the $ET4$ mono-model have an accuracy close to the mono-model $LW4$ in the laoded zone, differently the $ET4$ model reach a maximum value of the shear stress 9% lower than the reference $LW4$ solution. For multi-model theories the same comments made for the in-plane stress can be applied for the behaviour description of the transverse shear stress.
For transverse normal stress σ_{zz}, see Figure 13a, the mono-models $LW4$ and $ET4$ show the same accuracy solution. For multi-model theories the same comments made for the in-plane stress can be applied for the behaviour description of the transverse normal stress. It has to be noticed that the oscillations of the transition elements are smaller than those of the in-plane stress and the transverse shear stress.

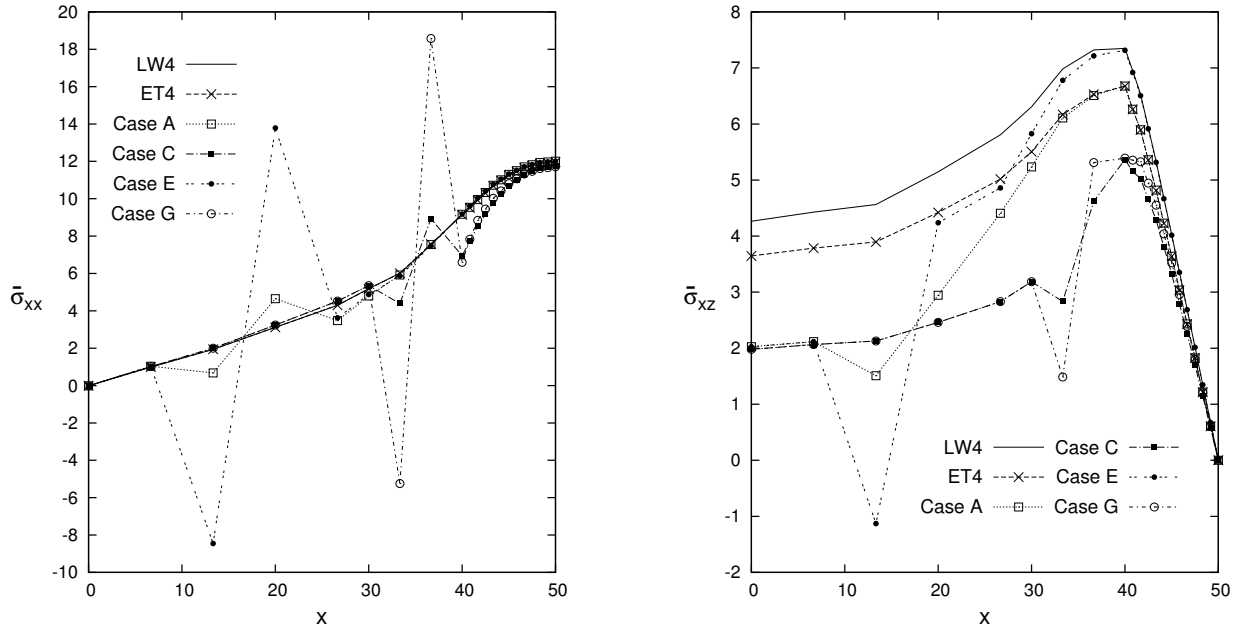

(a) σ_{xx} (b) σ_{xz}

Figure 12: Composite plate. In-plane stress $\sigma_{xx}(y;z) = \sigma_{xx}(b/2;-h/2)$, and transverse shear stress $\sigma_{xz}(y;z) = -10 \times \sigma_{xz}(b/2;0)$ along the in-plane direction X, the axis X is expressed in $[mm]$. Single and Multi-theory models.

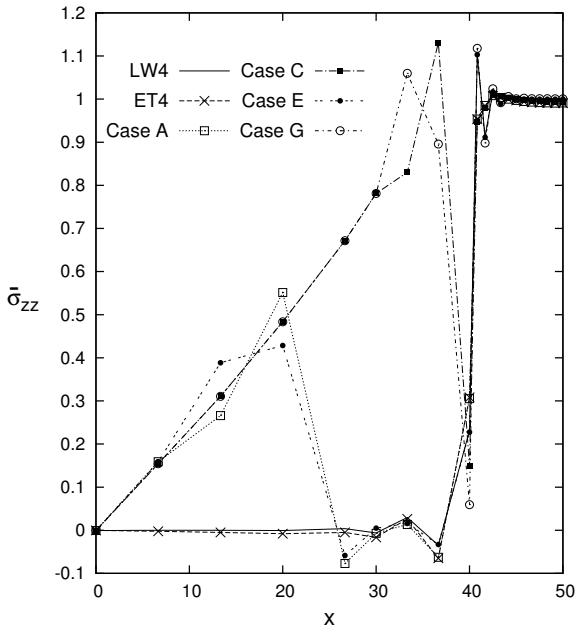

(a) σ_{zz}

Figure 13: Composite plate. Transverse normal stress $\sigma_{zz}(y;z) = -\sigma_{zz}(b/2;+h/2)$ along the in-plane direction X, the axis X is expressed in $[mm]$. Single and Multi-theory models.

Finally, a three-dimensional distributions on a quarter of the plate of the transverse shear stress σ_{xz} is given to underline the global/local capabilities of the presente finite element on the whole domain of

the analyzed plate structure. The reference single-model solution $LW4$ is depicted in Figure 14a. For a fair results comparison, the extremities of the colorbar values of the $LW4$ model are used to limit the colorbar of the other solutions. The single-model $ET4$ is not able to correctly describe the transverse shear stress behaviour, it is clear from Figure 14b that the interlaminar continuity of the transverse shear stress is not satisfied. In Figure 15a the multi-model named Case E, (ET1-LW4) is represented. It is evident that the transverse shear stress is well represented in the $LW4$ zone only. The multi-model Case H, (ET3-LW3) is represented in Figure 15b, the small $LW3$ zone is able to correctly describe the transverse shear stress, on the contrary the $ET3$ zone has a comparable behaviour as the single-model $ET4$.

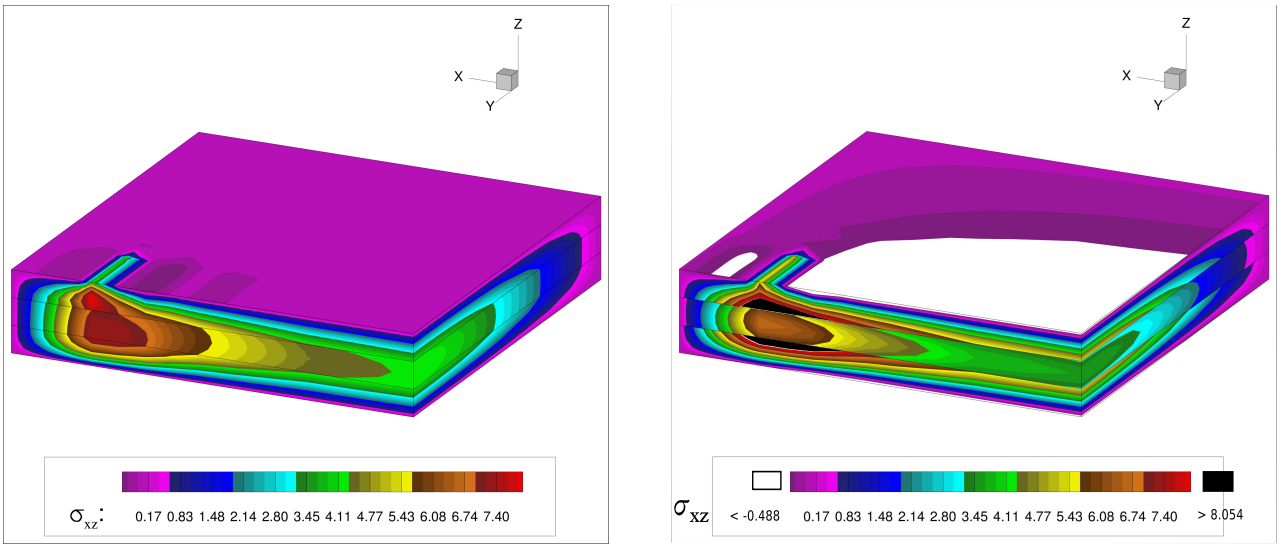

(a) $LW4$ (b) $ET4$

Figure 14: Composite plate, three-dimensional view of a quarter of the plate. Transverse shear stress σ_{xz} for single models.

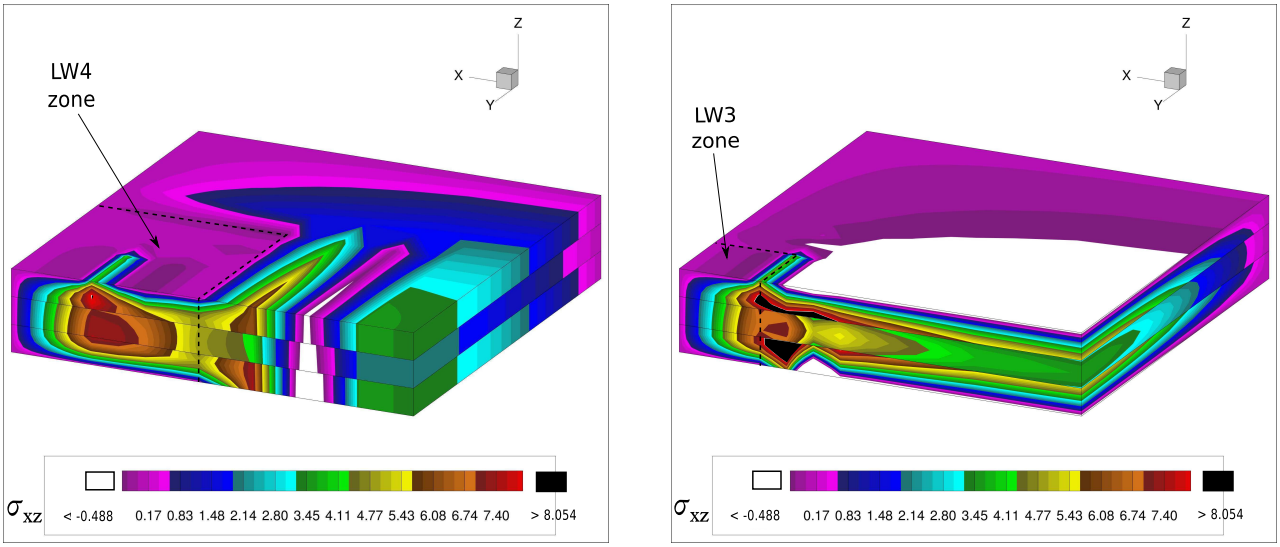

(a) Case E (b) Case H

Figure 15: Composite plate, three-dimensional view of a quarter of the plate. Transverse shear stress σ_{xz} for multi-models.

4.3 Sandwich rectangular plates simply-supported

A simply-supported unsymmetrically laminated rectangular sandwich plate is analysed. The geometrical dimensions are: $a = 100\,mm$, $b = 200\,mm$, the total thickness is $h = 12\,mm$, the top skin thickness is $h_{top} = 0.1\,mm$, the bottom skin is thick $h_{bottom} = 0.5\,mm$, and the core thickness is $h_{core} = 11.4\,mm$. The two skins have the same material properties: $E_1 = 70\,GPa$, $E_2 = 71\,GPa$, $E_3 = 69\,GPa$, $G_{12} = G_{13} = G_{23} = 26\,GPa$, $\nu_{12} = \nu_{13} = \nu_{23} = 0.3$, moreover the metallic foam core has the following material properties: $E_1 = E_2 = 3\,MPa$, $E_3 = 2.8\,MPa$, $G_{12} = G_{13} = G_{23} = 1\,MPa$, $\nu_{12} = \nu_{13} = \nu_{23} = 0.25$. The plate is simply-supported and a localised uniform transverse pressure, $P_z = -1\,MPa$, is applied at top face on a square region of side length equal to $(a = 5\,mm)\times(b = 20\,mm)$ and centered at the point $(a/2, b/2)$, see Figure 16.

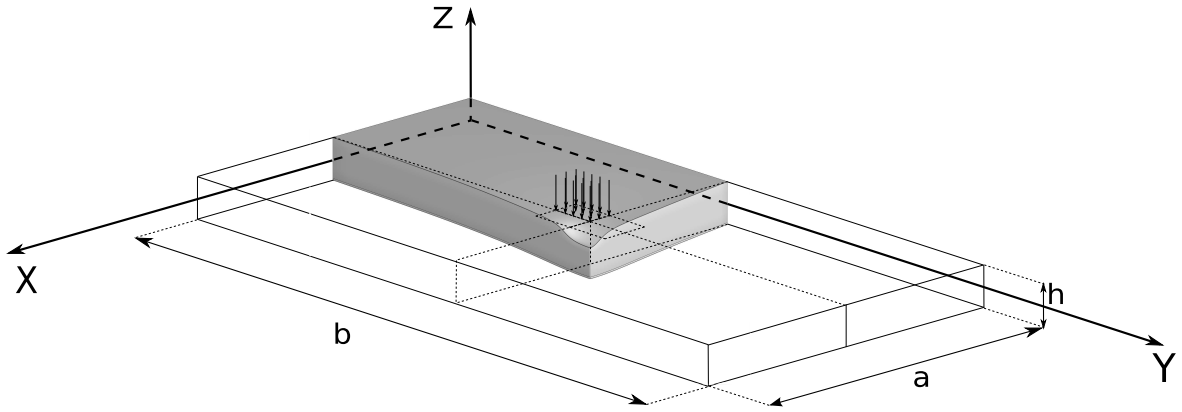

Figure 16: Reference system of the sandwich plate. Three-dimensional deflection representation of a quarter of the plate.

Due to the simmetry of both the geometry and the load, a quarter of the plate is analyzed and the following symmetry and boundary conditions (simply-supported) are applied:

$$\begin{array}{cccc} & \textit{Boundary} & & \textit{Simmetry} \\ u_s(x,0) = 0 & w_s(x,0) = 0 & & u_s(a/2,y) = 0 \\ v_s(0,y) = 0 & w_s(0,y) = 0 & & v_s(x,b/2) = 0 \end{array} \tag{19}$$

The present single- and multi-model solutions are compared with other soutions present in literature, three-dimensional analytical and three-dimensional FEM NASTRAN [67], ESL and LW analytical higher-order by the use of Fourier series expansions [68], ESL and LW FEM higher-order [69]. A non-uniform mesh grid of 38×54 elements ensures the convergence of the solution with a $LW4$ single-model, see Figure 17. For the sake of brevity the study of the convergence is here omitted. The adopted refined mesh is necessary to study the behaviour of the mechanical variables along the whole plate domain, and not in one single point. The difficult task is to obtain a good behaviour of the mechanical stresses, and in particular of the transverse normal stress σ_{zz} along the in-plane directions avoiding strange oscillations due to the changing of the element size.

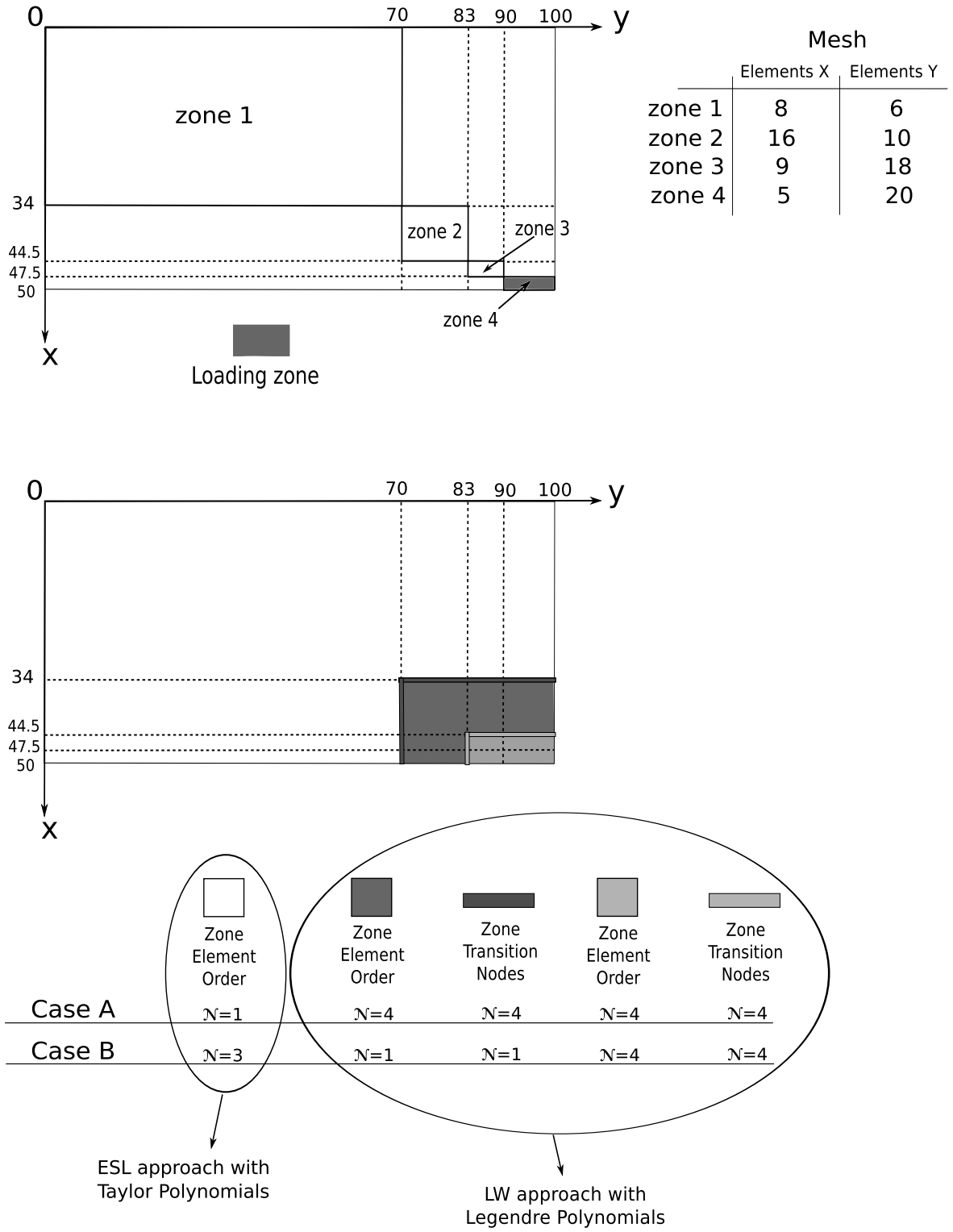

Figure 17: Non-uniform adopted mesh and graphical representation of the multi-model cases, for a quarter of the sandwich plate.

For the unsymmetrically laminated rectangular sandwich plate, mono-theory models are compared with those from the present global/local approach in Table 4. ESL models are not able to correct describe all the variables, therefore LW theories are necessary to match the reference analytical and

3D results. Table 4 also show solutions for variable kinematic multi-model theories. As emerged in the previous numerical sections, the primary variables (displacements) depend on the global domain approximation, in particular the transverse displacement w is better describe in the $Case\,B$ configuration with a $DOFs$ reduction of 34 % respect to the $Case\,A$ multi-model. On the contrary the postprocessed variables (stresses) are dependent on the local approximation.

Table 4: Unsymmetrically laminated rectangular sandwich plate. Transverse displacement w, in-plane normal stresses σ_{xx} and σ_{yy}, and transverse normal stress σ_{zz} evaluated at $(a/2, b/2)$ by various single- and multi-theory models.

	z	w	σ_{xx}	σ_{yy}	σ_{zz}	$DOFs$
			Top Skin			
3D Analytical [67]	Top	-3.78	-624	-241	-	
	Bottom		580	211	-	
3D NASTRAN [67]	Top	-3.84	-628	-237	-	
	Bottom		582	102	-	
LWM2 Analytical [68]	Top	-3.8243	-619.49	-	-	
	Bottom		577.36	-	-	
LWM2 FEM [69]	Top	-3.7628	-595.56	-223.93	-	
	Bottom		556.00	196.37	-	
			Top Skin			
$LW4$	Top	-3.7774	-622.48	-233.39	-0.9649	327327
	Bottom		578.60	203.25	-0.8738	
$LW3$	Top	-3.7723	-618.14	-232.33	-1.0143	251790
	Bottom		574.87	202.36	-0.8270	
$LW2$	Top	-3.7552	-601.46	-228.13	-0.9813	176253
	Bottom		559.72	198.73	-0.8710	
$LW1$	Top	-3.3896	-562.86	-286.15	-242.69	100716
	Bottom		530.98	262.78	240.82	
$ET4$	Top	-2.5498	-248.99	-38.930	256.87	125895
	Bottom		184.89	-1.7709	-275.80	
$ET3$	Top	-0.5995	-121.19	-56.428	-21.706	100716
	Bottom		59.439	8.9946	-19.349	
$ET2$	Top	-0.0238	-29.573	-28.178	-30.655	75537
	Bottom		-27.989	-27.470	-29.934	
$ET1$	Top	-0.0191	-29.740	-25.448	-25.404	50358
	Bottom		-29.444	-25.211	-25.248	
$Case\,A$	Top	-2.1386	-622.21	-220.95	-0.9649	245619
	Bottom		567.44	198.35	-0.8738	
$Case\,B$	Top	-2.4177	-609.14	-217.40	-0.9654	161007
	Bottom		563.79	196.16	-0.8663	

Some results in terms of transverse displacement w, and transverse normal stress σ_{zz} along the thickness of the sandwich plate are represented in Figures 18a, and 18b. The transverse displacement w behaviour can change sensitively depending on the distribution of the kinematic enrichment within the structure plane. Figure 18a show that ESL mono-models can vary sensitively their accuracy depending on the expansion order, differently the LW mono-models have almost the same accuracy independently

from the adopted expansion. Moreover for the multi-models, it is noticeable that the choice of the LW higher-order models for the loaded zone is not decisive for the correct description of the transverse mechanical displacement, as shown for $Case\,A$ and $Case\,B$.
On the other hand for the transverse normal stress σ_{zz}, see Figure 18b, LW higher-order models are able to correctly predict a good behaviour along the plate thickness. Multi-models theories $Case\,A$ and $Case\,B$ show the same accuracy of the reference solution $LW4$ in the considered evaluaton point.

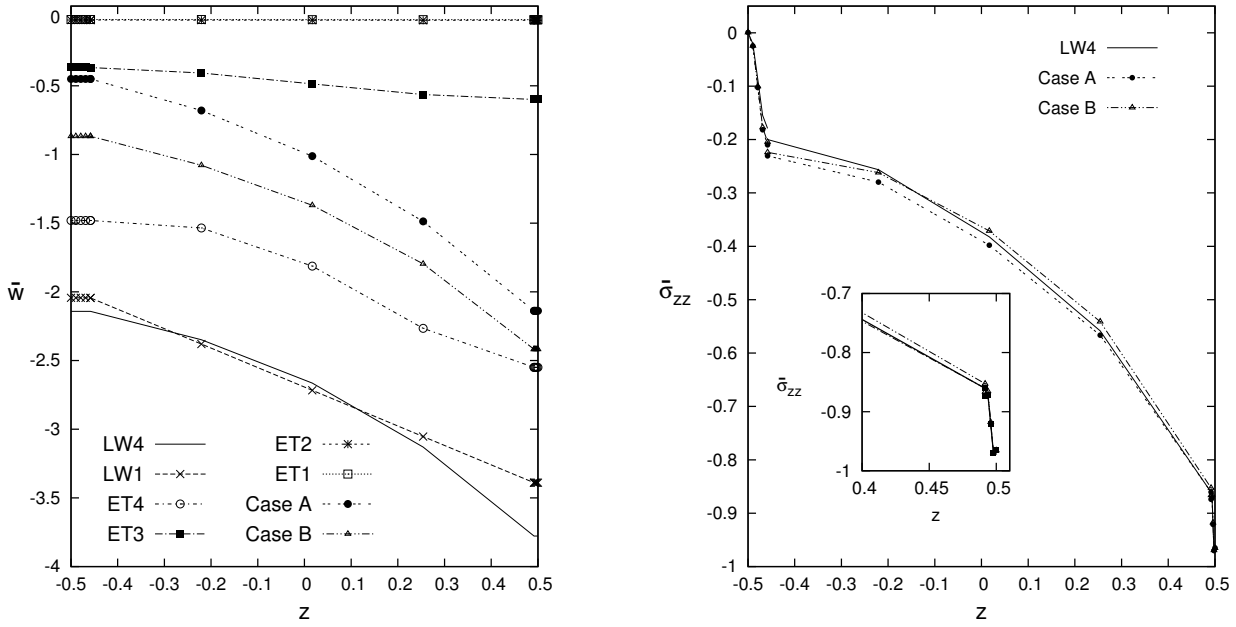

(a) w (b) σ_{zz}

Figure 18: Unsymmetrically laminated rectangular sandwich plate. Transverse displacement $w(x;y)$, and transverse normal stress $\sigma_{zz}(x;y)$ evaluated at $(a/2, b/2)$ by various single- and multi-theory models.

Results in terms of the three-dimensional representation of the in-plane stress σ_{xx} and its behaviour along the in-plane x axis are represented in Figures 19a and 19b respectively. In Figure 19a it is noticeable that the maximum values of the in-plane stress are located in the loading zone and its surroundings. Furthermore the behaviour of the in-plane stress σ_{xx} along the the in-plane x axis and evaluated at $(y, z) = (b/2, +h/2)$ is depicted in Figure 19b. Mono-models $LW4$ and $ET4$ and multi-models $Case\,A$ and $Case\,B$ show almost the same accuracy solution. Multi-models $Case\,A$ and $Case\,B$, produce small oscillations in the transition zone. It is noticeable that the oscillations are small, this is due to a finer mesh respect to the case of the previous numerical section.

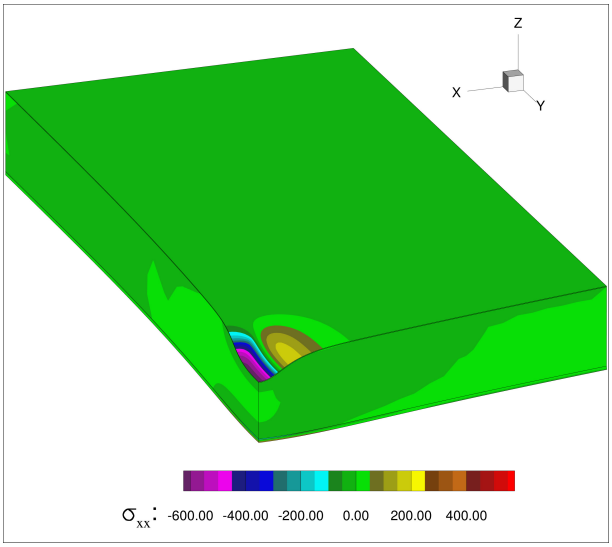

(a) $LW4$

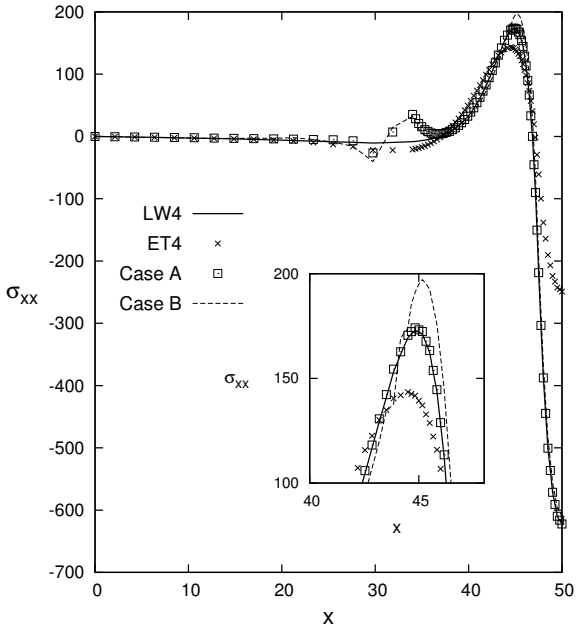

(b) Single and multi-models.

Figure 19: Unsymmetrically laminated rectangular sandwich plate. In-plane stress σ_{xx}, three-dimensional view of a quarter of the plate, and in-plane stress along the in-plane axis direction X evaluated at $(y, z) = (b/2, +h/2)$, for single and multi-models.

Finally, a three-dimensional distributions on a quarter of the sandwich plate of the transverse normal stress σ_{zz} is given to underline the global/local capabilities of the presente finite element on the whole domain of the analyzed sandwich plate structure. The reference single-model solution $LW4$ is depicted in Figure 20a. For a fair results comparison, the extremities of the colorbar values of the $LW4$ model are used to limit the colorbar of the other solutions. The single-model $ET4$ is not able to correctly describe the transverse shear stress behaviour, as shown in Figure 20b. Multi-model $Case\,A$ and $Case\,B$ are shown in Figures 21a and 21b respectively. It is evident that the transverse normal stress is well represented in the $LW4$ zone only, closed to the loaded zone.

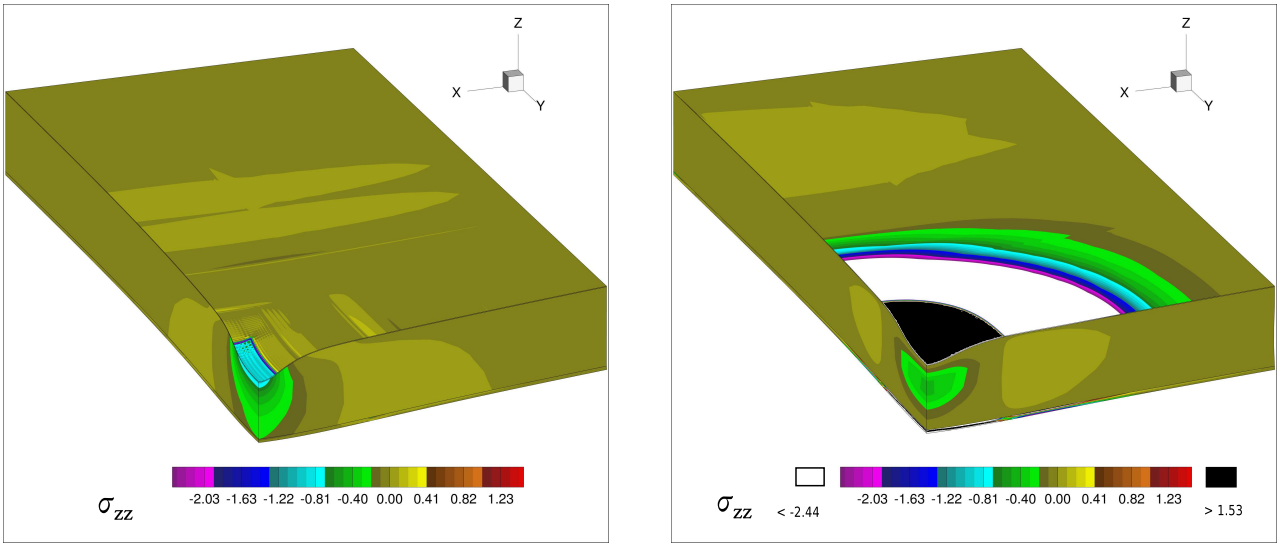

(a) $LW4$ (b) $ET4$

Figure 20: Unsymmetrically laminated rectangular sandwich plate, three-dimensional view of a quarter of the plate. Transverse normal stress σ_{zz} for single models.

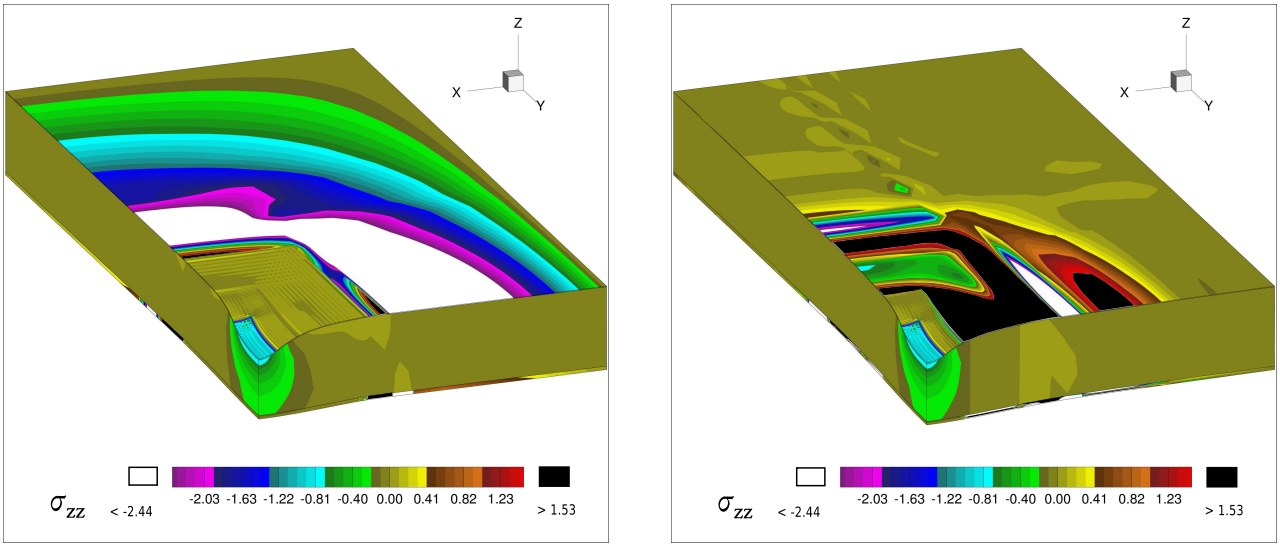

(a) Case A (b) Case B

Figure 21: Unsymmetrically laminated rectangular sandwich plate, three-dimensional view of a quarter of the plate. Transverse normal stress σ_{zz} for multi-models.

5 Conclusions

A new simultaneous multi-model approach for global/local analysis of composite and sandwich plates by means of a two-dimensional finite element with node-dependent kinematics has been introduced. The finite element governing equations are formulated in terms of *fundamental nuclei*, which are invariants of the theory approximation order. In this manner, the plate theory can vary within the same finite elements with no difficulties. No ad-hoc techniques and mathematical artifices are required to mix the fields coming from two different and kinematically incompatible adjacent zones, because the plate

structural theory varies within the finite element itself, therefore the same kinematics at the interface nodes between kinematically incompatible plate elements is enforced. The proposed methodology has been widely assessed in this work by analysing composite and sandwich plates and by comparison with analytical, FEM and 3D solid commercial solutions from the literature. Furthermore, it has been demonstrated that refined 2D models are able to detect complex strain-stress fields, in accordance with more cumbersome 3D models. Accurate results have been obtained in the refined part of the model with a significant reduction of the total number of degrees of freedom and, therefore, of the computational cost. Future developments will deal with the extension of this global/local methodology to hierarchical shell theories and to the Reissner Mixed Variational Theorem (RMVT).

References

[1] W T Koiter. On the foundations of the linear theory of thin elastic shell. *Proc. Kon. Nederl. Akad. Wetensch.*, 73:169–195, 1970.

[2] P G Ciarlet and L Gratie. Another approach to linear shell theory and a new proof of Korn's inequality on a surface. *C. R. Acad. Sci. Paris*, I,340:471–478, 2005.

[3] E Reissner and Y Stavsky. Bending and stretching of certain types of heterogeneous aelotropic elastic plates. *Journal of Applied Mechanics*, 28:402–408, 1961.

[4] E Reissner. The effect of transverse shear deformation on the bending of elastic plates. *Journal of Applied Mechanics*, 12(2):69–77, 1945.

[5] R D Mindlin. Influence of rotary inertia and shear flexural motion of isotropic, elastic plates. *Journal of Applied Mechanics*, 18:31–38, 1951.

[6] T Kant, D R J Owen, and O C Zienkiewicz. Refined higher order C^0 plate bending element. *Computer & Structures*, 15:177–183, 1982.

[7] T Kant and J R Kommineni. Large amplitude free vibration analysis of cross-ply composite and sandwich laminates with a refined theory and C^0 finite elements. *Computer & Structures*, 50:123–134, 1989.

[8] J N Reddy. Mechanics of laminated composite plates and shells. *Theory and Analysis, CRC Press*, 1997.

[9] A N Palazotto and S T Dennis. Nonlinear analysis of shell structures. *AIAA Series*, 1992.

[10] A K Noor and W S Burton. Assessment of computational models for multi-layered composite shells. *Applied Mechanics Review*, 43:67–97, 1990.

[11] J N Reddy. An evaluation of equivalent-single-layer and layerwise theories of composite laminates. *Composite Structures*, 25:21–35, 1993.

[12] A S Mawenya and J D Davies. Finite element bending analysis of multilayer plates. *Journal for Numerical Methods in Engineering*, 8:215–225, 1974.

[13] F G Rammerstorfer, K Dorninger, and A Starlinger. Composite and sandwich shells. *Nonlinear Analysis of Shells by Finite Elements*, 328:131–194, 1992.

[14] R E Bank. Adaptive computational methods for partial differential equations. *SIAM*, 1983.

[15] B A Szabo and I Babuska. Finite element analysis. *John Wiley & Sons*, 1991.

[16] K J Bathe. Finite element procedure. *Prentice Hall*, 1996.

[17] D M Thompson and O H Jr Griffin. 2-D to 3-D Global/Local Finite Element Analysis of Cross-Ply Composite Laminates. *Journal of Reinforced Plastics and Composites*, 9:492–502, 1990.

[18] K M Mao and C T Sun. A Refined Global-Local Finite Element Analysis Method. *International Journal for Numerical Methods in Engineering*, 32:29–43, 1991.

[19] J D Whitcomb and K Woo. Application of Iterative Global/Local Finite Element Analysis. Part 1: Linear Analysis. *Communications in Numerical Methods in Engineering*, 9(9):745–756, 1993.

[20] J D Whitcomb and K Woo. Application of Iterative Global/Local Finite Element Analysis. Part 2: Geometrically Non-Linear Analysis. *Communications in Numerical Methods in Engineering*, 9(9):757–766, 1993.

[21] A S D Wang and F W Crossman. Calculation of Edge Stresses in Multi-Layer by Sub-Structuring. *Journal of Composite Materials*, 12:76–83, 1978.

[22] N J Pagano and S R Soni. Global-Local Laminate Variational Model. *International Journal of Solids and Structures*, 19(3):207–228, 1983.

[23] R Jones, R Callinan, K K Teh, and K C Brown. Analysis of Multi-Layer Laminates Using Three-Dimensional Super Elements. *International Journal for Numerical Methods in Engineering*, 20(3):583–587, 1984.

[24] A Pagani, S Valvano, and E Carrera. Analysis of laminated composites and sandwich structures by variable-kinematic MITC9 plate elements. *Journal of Sandwich Structures and Materials*. In Press. DOI: 10.1177/1099636216650988.

[25] E Carrera, A Pagani, and S Valvano. Shell elements with through-the-thickness variable kinematics for the analysis of laminated composite and sandwich structures. *Composites Part B*, 111:294–314, 2017.

[26] E Carrera and S Valvano. A variable kinematic shell formulation applied to thermal stress of laminated structures. *Journal of Thermal Stresses*. In Press. DOI: 10.1080/01495739.2016.1253439.

[27] F Brezzi and L D Marini. The three-field formulation for elasticity problems. *GAMM Mitteilungen*, 28:124–153, 2005.

[28] E Carrera, A Pagani, and M Petrolo. Use of Lagrange multipliers to combine 1D variable kinematic finite elements. *Computers & Structures*, 129:194–206, 2013.

[29] E. Carrera and A. Pagani. Analysis of reinforced and thin-walled structures by multi-line refined 1D/beam models. *International Journal of Mechanical Sciences*, 75:278–287, 2013.

[30] E. Carrera and A. Pagani. Multi-line enhanced beam model for the analysis of laminated composite structures. *Composites: Part B*, 57:112–119, 2014.

[31] H Ben Dhia. Multiscale mechanical problems: the Arlequin method. *Comptes Rendus de l'Academie des Sciences Series IIB Mechanics Physics Astronomy*, 326(12):899–904, 1998.

[32] H Ben Dhia. Numerical modelling of multiscale problems: the Arlequin method. *CD Proceedings of ECCM'99, Munchen*, 1999.

[33] H Ben Dhia. Further insights by theoretical investigations of the multiscale Arlequin method. *International Journal for Multiscale Computational Engineering*, 6(3):215–232, 2008.

[34] H Ben Dhia. he Arlequin method as a flexible engineering tool. *International Journal for Numerical Methods in Engineering*, 62(11):1442–1462, 2005.

[35] H Hu, S Belouettar, M Potier-Ferry, and E M Daya. Multi-scale modelling of sandwich structures using the Arlequin method. Part I: linear modelling. *Finite Elements in Analysis and Design*, 45(1):37–51, 2008.

[36] H Hu, S Belouettar, M Potier-Ferry, E M Daya, and A Makradi. Multi-scale nonlinear modelling of sandwich structures using the Arlequin method. *Finite Elements in Analysis and Design*, 92(2):515–522, 2010.

[37] F Biscani, G Giunta, S Belouettar, E Carrera, and H Hu. Variable kinematic beam elements coupled via Arlequin method. *Composite Structures*, 93(2):697–708, 2011.

[38] F Biscani, G Giunta, S Belouettar, E Carrera, and H Hu. Variable kinematic plate elements coupled via Arlequin method. *International Journal for Numerical Methods in Engineering*, 91:1264–1290, 2012.

[39] J N Reddy and D H Robbins. Theories and computational models for composite laminates. *Applied Mechanics Review*, 47:147–165, 1994.

[40] Junuthula N Reddy. Mechanics of laminated composite plates- Theory and analysis(Book). *Boca Raton, FL: CRC Press, 1997.*, 1997.

[41] J Fish. The s-version of the finite element method. *Computers and Structures*, 43(3):539–547, 1992.

[42] J Fish and S Markolefas. Adaptive s-method for linear elastostatics. *Computer Methods in Applied Mechanics and Engineering*, 103:363–396, 1993.

[43] C Wenzel, P Vidal, M D'Ottavio, and O Polit. Coupling of heterogeneous kinematics and Finite Element approximations applied to composite beam structures. *Composite Structures*, 116:177–192, 2014.

[44] E Carrera, A Pagani, and S Valvano. Multilayered plate elements accounting for refined theories and node-dependent kinematics. *Composites Part B*, 114:189–210, 2017.

[45] K J Bathe and E Dvorkin. A formulation of general shell elements - the use of mixed interpolation of tensorial components. *International Journal for Numerical Methods in Engineering*, 22:697–722, 1986.

[46] K J Bathe and F Brezzi. A simplified analysis of two plate bending elements-the MITC4 and MITC9 elements. *Proceedings, Numerical Methods in Engineering: Theory and Applications*, 1987.

[47] K J Bathe, F Brezzi, and S W Cho. The MICT7 and MITC9 plate bending elements. *Computers & Structures*, 32(3-4):797–814, 1989.

[48] M L Bucalem and E Dvorkin. Higher-order MITC general shell elements. *International Journal for Numerical Methods in Engineering*, 36:3729–3754, 1993.

[49] E Carrera, M Cinefra, and E Petrolo M. abd Zappino. *Finite Element Analysis of Structures through Unified Formulation*. John Wiley & Sons, 2014.

[50] E Carrera and S Brischetto. Analysis of thickness locking in classical, refined and mixed multilayered plate theories. *Composite Structures*, 82:549–562, 2008.

[51] E Carrera. Theories and finite elements for multilayered plates and shells: a unified compact formulation with numerical assessment and benchmarking. *Archives of Computational Methods in Engineering*, 10(3):215–296, 2003.

[52] E Carrera. Multilayered shell theories accounting for layerwise mixed description, Part 1: governing equations. *AIAA Journal*, 37(9):1107–1116, 1999.

[53] E Carrera. Multilayered shell theories accounting for layerwise mixed description, Part 2: numerical evaluations. *AIAA Journal*, 37(9):1117–1124, 1999.

[54] M Cinefra, S Valvano, and E Carrera. Heat conduction and Thermal Stress Analysis of laminated composites by a variable kinematic MITC9 shell element. *Curved and Layered Structures*, 1:301–320, 2015.

[55] M Cinefra, S Valvano, and E Carrera. Thermal Stress Analysis of laminated structures by a variable kinematic MITC9 shell element. *Journal of Thermal Stresses*, 39(2):121–141, 2016.

[56] Maria Cinefra, Erasmo Carrera, and Stefano Valvano. Variable Kinematic Shell Elements for the Analysis of Electro-Mechanical Problems. *Mechanics of Advanced Materials and Structures*, 22(1-2):77–106, September 2015.

[57] M Cinefra, S Valvano, and E Carrera. A layer-wise MITC9 finite element for the free-vibration analysis of plates with piezo-patches. *International Journal of Smart and Nano Materials*, 6(2):85–104, 2015.

[58] E. Carrera. Historical review of Zig-Zag theories for multilayered plates and shells. *Applied Mechanics Reviews*, 56:287–308, 2003.

[59] E. Carrera. On the use of the Murakami's zig-zag function in the modeling of layered plates and shells. *Computers and Structures*, 82:541–554, 2004.

[60] E. Carrera. Mixed layer-wise models for multilayered plates analysis. *Composite Structures*, 43:57–70, 1998.

[61] E. Carrera. Evaluation of Layerwise Mixed Theories for Laminated Plates Analysis. *Applied Mechanics Reviews*, 36(5):830–839, 1998.

[62] S G Lekhnitskii. Anisotropic Plates. In *Tsai, S W and Cheron, T editors (Translated from 2nd Russian Edition)*. Gordon & Branch, 1968.

[63] S H Nguyen and K S Surana. Two-dimensional curved beam element with higher-order hierarchical transverse approximation for laminated composites. *Computers & Structures*, 36:499–511, 1990.

[64] J F Davalos, Kim Y, and Barbero E J. Analysis of laminated beams with a layerwise constant shear theory. *Computers & Structures*, 28:241–253, 1994.

[65] Y Z Xiaoshan Lin. A novel one-dimensional two-node shear-flexible layered composite beam element. *Finite Elements in Analysis and Design*, 47:676–682, 2011.

[66] T P Vo and H T Thai. Static behavior of composite beams using various refined shear deformation theories. *Computers & Structures*, 94:2513–2522, 2012.

[67] H R Meyer-Piening. Experiences with 'exact' linear sandwich beam and plate analyses regarding bending, instability and frequency investigations. In *Proceedings of the Fifth International Conference on Sandwich Constructions, Vol. 1, edited by H.R. Meyer-Piening and D. Zenkert*, pages 37–48, EMAS Publishing, Zurich, 2000.

[68] E Carrera and A Ciuffreda. Bending of composites and sandwich plates subjected to localized lateral loadings: a comparison of various theories. *Composite Structures*, 68:185–202, 2005.

[69] E Carrera and L Demasi. Two benchmarks to assess two-dimensional theories of sandwich, composite plates. *AIAA Journal*, 41(7):1356–1362, 2003.